UNIVESITY OF CALIFORNIA
RIVERSIDE

Development of High-Throughput and Real-Time Methods for the Detection of Infectious Enteric Viruses

A Dissertation submitted in partial satisfaction
of the requirements for the degree of

Doctor of Philosophy

in

Chemical and Environmental Engineering

by

Hsiao-Yun Yeh

June 2010

Dissertation Committee:
Dr. Wilfred Chen, Chairperson
Dr. Ashok Mulchandani
Dr. Marylynn V. Yates

The Dissertation of Hsiao-Yun Yeh approved:

_____

_____

_____

Committee chairperson

University of California, Riverside

Acknowledgements

I would like to express my gratitude to Professor Wilfred Chen, Professor Marylynn V. Yates, and Professor Ashok Mulchandani, for their support and advice in developing this dissertation. I am particularly grateful for their sharing of perspective on researches and life with me. I also want to acknowledge financial support from the U.S. Environmental Protection Agency STAR grant program (R833008). I am thankful to publishers of the journals for their permission to reprint the papers

1. Hsiao-Yun Yeh, Marylynn V. Yates, Ashok Mulchandani, and Wilfred Chen. Molecular beacon-quantum dot-Au nanoparticle hybrid nanoprobes for visualizing virus replication in living cells, *Chem. Comm.*, Accepted for Publication, 2010.
2. Hsiao-Yun Yeh, Marylynn V. Yates, Wilfred Chen, and Ashok Mulchandani. Real-time molecular methods to detect infectious viruses: a mini-review. *Seminars in Cell & Developmental Biology*, 20, 49-54, 2009. (Invited Contribution)
3. Hsiao-Yun Yeh, Marylynn V. Yates, Ashok Mulchandani, and Wilfred Chen. Visualizing the dynamics of viral replication in living cells via Tat-peptide delivery of nuclease-resistant molecular beacons. *Proc. Natl. Acad. Sci. USA*, 105, 17522-17525, 2008.
4. Hsiao-Yun Yeh, Yu-Chen Hwang, Marylynn V. Yates, Ashok Mulchandani, and Wilfred Chen. Detection of hepatitis A virus by using a combined cell culture – molecular beacon assay. *Appl. Environ. Microbiol.*, 74, 2239-2243, 2008,

that appear in these journals and form a part of this dissertation.

ABSTRACT OF THE DISSERTATION

Development of High-Throughput and Real-Time Methods
for the Detection of Infectious Enteric Viruses

by

Hsiao-Yun Yeh

Doctor of Philosophy
Chemical and Environmental Engineering
University of California, Riverside, June 2010
Dr. Wilfred Chen, Chairperson

Waterborne transmitted viruses pose a public health threat due to their stability in aquatic environments and their ease of transmission with high morbidity rates at low infectious doses. The ability to detect infectious viruses is of critical importance for environmental health and safety. Current methods to assess the presence of infectious viruses are based on detecting the production of cytopathic effects from mammalian cell culture and can take up to weeks before positive identification. Improved methods for rapid and reliable detection and population quantification of infectious viruses are needed for public health assessments. Molecular beacons (MBs), which produce fluorescence upon target binding, provide a simple and separation-free scheme for rapid and sensitive detection of infectious viruses. However, for real-time studies in living cells, the durability of MBs is affected by the intracellular nuclease degradation. Additionally, cell fixation and permeabilization are required to maintain the cellular structure before introducing MBs. In this study, we developed several FRET (fluorescence resonance energy transfer)-based MBs combined with fluorescence microscopy to directly visualize the fluorescent hybrids with newly synthesized viral RNA as an indication of viral

infection and to subsequently follow virus spread among cells *in situ/in vivo*. To prevent nucleolytic degradation, we designed MBs containing 2′-O-methyl RNA bases with phosphorothioate internucleotide linkages, which specifically target the 5′ noncoding region of the viral genome. A cell-penetrating Tat peptide was appended to the FRET probes to facilitate non-invasive entry into host cells. To further improve the probe sensitivity in providing real-time and long-term detection of viral replication, MBs composed of quantum dot and gold nanoparticles were generated. Confluent cell monolayers were incubated with the probes followed by infection with virus dilutions and the fluorescence intensity was monitored in real time. Sensitivity experiments showed that 1 PFU detection limit could be achieved within one replicative cycle. The illumination of fluorescent cells increased in a dose-responsive manner and enabled the direct quantification of infectious viral doses. By introducing the modified MBs into the host cell population prior to viral infection and tracking the change of fluorescence signals, we observed cell-to-cell spread when progeny virions infected new host cells in which the infectious cycle could be repeated. The specific nature of these probes enable their utility for rapid diagnostics of viral infections and real-time viral detection *in vivo* provides sufficient information regarding multiple steps in infection processes at the subcellular level, which will be valuable for the prevention, control, and understanding of viral infection.

Table of Contents

Table of Figures

Chapter 1:

Introduction

Introduction

Environmental virology initiated with scientists attempting to detect poliovirus more than half a century ago (1). In the United States, waterborne disease outbreaks were associated with treatment deficiencies in water supply and distribution system contamination (2). Close to 50% of all waterborne disease outbreaks are due to acute gastrointestinal illness (AGI) caused by agents of undetermined etiology (3). Given the specimen collection limitations and disease patterns, it is reasonable to speculate that most of the unknown agents may be of viral origin. Among the identified etiologic agents, the presence of human enteric viruses in water such as enteroviruses, astroviruses, hepatoviruses, rotaviruses, Norwalk and related caliciviruses, have accounted for more than half of the outbreaks and worldwide epidemics (2, 4–7).

According to US centers for disease control and prevention, human enteric viruses are mainly transmitted by the fecal-oral route, such as through ingestion of contaminated food or water. Poliovirus is the causative agent of poliomyelitis (often called polio or infantile paralysis). The non-polio enteroviruses (e.g. coxsackie A/B viruses, echoviruses) cause a variety of clinical syndromes, including gastroenteritis, viral meningitis, myocarditis, encephalitis, and diabetes mellitus. Hepatoviruses cause acute liver infection. Four of the human enteric virus, coxsackievirus, echovirus, calicivirus, and adenovirus, have been included among the microorganisms of concern on the Environmental Protection Agency's (EPA) Drinking Water Contaminant Candidate List (CCL) (8). The importance of water as a vehicle for virus transmission, coupled with low

infectious doses prompt the urgent need for rapid and reliable methods to detect small numbers of infectious virus particles in environmental samples.

Conventionally, immunological, nucleic acid-based, and infectivity-based (cell culture) methods, have been applied as molecular techniques for virus analysis (1, 7, 9–13). Immunological and nucleic acid-based methods determine only the total virus particle number and do not stress the discrepancy between the presence of physical virus particles (irrespective of its ability to infect cells and reproduce) and viable virus (1, 7). The only reliable method to detect infectious viruses is based on mammalian cell culture, which detects the production of visible cytopathic effects (CPE). This method is difficult to perform and may take weeks before the viruses reach measurable amounts to allow detection. Epidemiologically important viruses that cannot be grow in cell culture or grown with difficulty, e.g. adenovirus type 40 and 41, astrovirus, and caliciviruses, have prompted the need for new detection approaches that are rapid, sensitive and specific. These approaches must be quantitative and can preclude the detection of non-infectious viruses.

This thesis presents the research for development of high-throughput and real-time methods for the detection of infectious enteric viruses. We are interested in using nuclease-resistant and photodegradation-resistant molecular beacon-based DNA-probes to target infectious viruses, especially highlighting the key issues pertaining to overcoming the main difficulties such as occurrence of low infectious viral particle numbers (particularly in the water environment), and the technical challenges of virus assays. Our proposal includes: (i) probe backbone modification by combining 2'-O-

methyl RNA bases with phosphorothioate internucleotide linkages for resisting nuclease degradation, (ii) an attachment of the Tat peptide to the probe, to facilitate entry into host cells without permeabilization, and (iii) design molecular beacons composed of quantum dots and gold nanoparticles as FRET (fluorescence resonance energy transfer) pairs for improved sensitivity and possibly multiplexing capability. The objective is to develop high-throughput real-time detection and quantification for infectious viruses in the cell population and to investigate the durability of the probes for providing real-time and long-term *in vivo* monitoring of viral infection, viral replication, and for viral quantification.

Current Methods of Viral Detection

Scientists have been making progress in viral detection methods over the past 60 years. The advent of molecular biology further leads to the development of new approaches for meeting current challenges and has expanded our knowledge of viral structures and functions at the molecular level. A variety of experimental techniques, e.g. immuno-affinity, nucleic acid-based or cell culture-based detection, have already been employed to measure the presence of virus or viral infection. Immunological (serological) methods such as radioimmunoassay, immunofluorescence, immune electron microscopy or enzyme-linked immune-sorbent assay (ELISA) are based on the interaction between a viral antigen and an antibody; the capture antibody directs against the viral antigen and the bound complex are detected via chromogenic or fluorogenic molecules. The detection limit varies by the variability of the viral genome and the affinity of antibody interaction. Immunological methods require sophisticated apparatus and specialized training, and they generally lack the degree of sensitivity required to detect the low quantities of viruses expected in environmental samples (1, 7).

Substantial improvements in sensitivity over conventional molecular techniques have been achieved by nucleic acid-based amplification methods such as polymerase chain reaction (PCR), reverse transcription-PCR (RT-PCR), or quantitative real-time PCR (qRT-PCR) (9–12). The employment of PCR-based methods for viral detection and quantification provides the benefit of rapid analysis with high sensitivity and reproducibility at relatively low cost. However, the major obstacles include: (i) environmental inhibitors (e.g. humic compounds) concentrated along with viruses during

water sample processing, (ii) the small volume assayed may lead to false-negative results because of the low virus titers; and (iii) PCR or RT-PCR may yield false-positive results by detecting noninfectious or inactivated viruses, suggesting that a positive result may not necessarily pose a public health threat.

PCR amplification can be combined with other molecular technologies, e.g. *in situ* hybridization (ISH) (14, 15), microarray (16), or cell culture, to maximize sensitivity and specificity in the detection of known waterborne pathogenic viruses. For example, ISH can localize and determine the relative abundance of specific DNA or RNA sequences in infected cells that are fixed on a glass slide. Fluorescence *in situ* hybridization (FISH) can be used in viral diagnostics to assess chromosomal integrity and to help the identification of viruses. To detect the low viral copy sequences, the assay sensitivity maybe improved by *in situ* RT-PCR or PCR (14, 15, 17, 18). Studies have shown that *in situ* RT-PCR (*in situ* PCR) allows for the detection of RNA sequences of infectious bursal disease virus and human papillomavirus DNA with copy numbers below the detection threshold of conventional ISH analysis (19, 20).

DNA microarray has become an alternate hybridization method for the analysis of cellular gene expression in response to viral infection. In general, microarrays are miniaturized arrays of locations on a solid surface such as a glass microscope slide or a silicon chip in aligned rows. The DNA sequences attached to a microarray are used as probes to capture their corresponding fluorophore-labeled DNA targets. Probe-target hybridization can be quantified by fluorescence-based detection to determine the relative abundance of the targets. Recently, a foot and mouth disease virus (FMDV) microarray

was described to simultaneously detect seven FMDV serotypes. The results encourage the development of new oligonucleotide microarrays to probe the differences in the genetic and antigenic composition of FMDV, and to gain insight into the molecular epidemiology of this pathogen (21). Using the fully sequenced viral genomic data, a highly conserved oligonucleotide DNA microarray is capable of simultaneously detecting and identifying diverse viruses by the unique pattern of hybridization generated by each virus. Perhaps equally important to the detection of viral pathogens, the viral genomic and microarray-based strategy has the potential to facilitate the determination of viral subtypes and to identify diseases of unknown etiology (16, 22). A subtyping assay for both the hemagglutinin and neuraminidase surface antigens of the avian influenza viruses has been developed using padlock probes to form circular molecules when paired to the appropriate target (22). The circular probes are amplified by a rolling-circle amplification and PCR, and when combined with a microarray output for detection, this assay is capable of differentiating among all known surface antigen subtypes within 4 h. Viral microarray design can further use the Protein Families database, protein-motif (subjected to coding sequences) and nucleic acid motif (subjected to non-coding sequences) finding algorithms to ensure a nearly complete coverage of the related viral sequence database (23).

The major drawback to most current methods is that they are usually used to approximate the quantity of viruses present in a sample but do not provide information whether a pathogen has the ability to establish an infection or not. To overcome this problem, the infectious assays may be achieved by cell culture techniques with the

appropriate cell line in conjunction with other developed methods for direct assessment of infectious virus. For example, cell culture followed by RT-PCR probe the specific viral mRNA present in the cell during viral replication. Propagation of cultivable virus in host cells generates enough progeny viruses to enable ready detection by the nucleic acid-based test (13). However, this method requires additional mRNA extraction, RT-PCR reactions, and gel analysis, leading to added analysis time and the potential for contamination. Cell culture method remains the gold standard for virus diagnosis because it is the only method available for detecting infectious viral particles and can achieve a detection limit of 1 plaque forming unit (PFU) per volume (7). However, some health-significant viruses such as astrovirus or norovirus still cannot be cultivated or grow poorly in cell culture (17, 24). Certain viruses like hepatovirus and adenovirus have been reported that the viral replication is relatively slow and causes ambiguous CPEs in cell culture (25, 26). New cell lines need to be investigated for those non-culturable but epidemiologically important viruses.

The study of norovirus, a major cause for foodborne gastroenteritis outbreaks, has been complicated by recombination between strains and the lack of an *in vitro* culture system with high yield. Recently, a complicated norovirus cell culture model has been reported for an infectivity assay that infects and replicates in a 3D human small intestinal epithelium (17). This breakthrough may provide insights into the molecular biology of norovirus, such as viral attachment and intracellular replication, in addition to the genomic and proteomic profiling. Alternative steps that depend on functional components of the virus needed for infection may be employed as an additional approach to detect

only infectious viruses. Methods include the specific capture of virus by cellular receptors for virus *in vitro* followed by molecular detection of viral nucleic acid in the captured virus (27).

Emerging Tools for Real-Time Monitoring of Viral Replication

Real-time detection of the viral load in living cells provides information on the dynamics of proliferation of the infectious pathogen and has prognostic relevance in a number of clinical studies that can serve as a basis for guiding therapeutic interventions. In particular, the ability to monitor the real-time replication of viruses in living cells are vital for the rapid detection of viral infection and understanding of viral pathogenesis. Among the technologies currently under development for gene detection in living cells, the most promising one is perhaps molecular beacons (MBs). MBs provide a label-based and separation-free detection scheme and the specificity and sensitivity of MBs have led to their use in numerous *in vitro* hybridization assays (28–31). They are single-stranded oligonucleotide probes possessing a stem-loop structure and are double labeled with a fluorophore at one arm and a quencher at the other. In the absence of the complementary target sequence, the quencher will absorb any photons emitted by the fluorophore through fluorescence resonance energy transfer. Fluorescence resonance energy transfer (FRET) is a process involving the radiation-less transfer of energy from a donor fluorophore to an appropriately positioned acceptor fluorophore. The illumination of the donor fluorophore results in increased fluorescence emission from the acceptor. Three criteria need to be satisfied for FRET to occur: spectral, dipole orientation, and distance. FRET can occur when the emission spectrum of a donor fluorophore significantly overlaps (> 30%) the absorption spectrum of an acceptor, provided that the donor and acceptor fluorophores dipoles are in favorable mutual orientation (approximately parallel). Because the efficiency of energy transfer varies inversely with (the sixth power of) the distance

separating the donor and acceptor fluorophores, the distance over which FRET can occur is limited to between 1-10 nm. In the presence of a complementary sequence, the beacon undergoes a conformational change; it unwinds and binds to the target. The fluorophore moves away from the quencher, restoring fluorescence upon probe-target hybridization.

These probes are specific for a target nucleotide sequence and produce fluorescence upon target binding. The spontaneous hybridization between MBs and their target sequences is highly specific and can even distinguish a single nucleotide mismatch (32–34). The reported MB-based reverse-transcription-PCR (RT-PCR) provided sensitive and specific detection of hepatitis A virus and as few as 1 PFU was detected (35). Recently, MBs have been used to detect the presence of viral RNAs in infected cells with positive responses to even one single infectious viral particle (Fig. 1.1) (36, 37). By labeling endogenous RNA with MBs, the dynamic behavior of poliovirus (+) strand RNA in living host cells have also been studied (38).

Although MBs have the potential to become a powerful real time tool to monitor and quantify the level of infectious virus in living cells, the major challenge in using conventional MBs *in vivo* is the relative short half-life (~50 min) of MBs due to cytoplasmic degradation. This could dramatically decrease the MBs' sensitivity by digesting the deoxyribonucleotide backbone and disrupting the stem-loop structure, resulting in false-positive fluorescence signals unrelated to MB/target hybridization (39, 40). Moreover, upon target binding, the RNA–DNA duplex region is susceptible to cellular RNase H activity; the RNase H cleavage results in false-negative signals due to the degradation of the bound RNA (41). To maintain the stability of MB structure, many

attempts, such as 2'-O-methyl modifications and phosphorothioate internucleotide linkages, can be made to increase duplex stability and nuclease resistance, as well as to have a higher affinity and coupling efficiency (42–45). The rationale for using nuclease-resistant MBs to detect viral RNAs in living cells is to improve signal-to-noise ratios by eliminating false-positive and false-negative fluorescence signals derived from endogenous nuclease degradation.

In addition to the short half-life, real-time monitoring of viral replication is hampered by the lack of an efficient and non-invasive method for intracellular delivery of fluorescent probes. The *in situ* hybridization with MBs requires permeabilization for MB molecules to enter the cell's interior and cell fixation prior to microscopy observations; the pre-treatments make the *in vivo* localization of mRNA/RNA or real-time detection of viral replication impossible. Endocytic approaches such as transfection are slow and the probes are predominately trapped inside endosomes and lysosomes (46). Even microinjection is not suitable for viral detection because it is difficult to predict which cells are infected "*a priori*". Cellular uptake based on streptolysin O is faster (~2 h) but can only be used in *ex vivo* cellular assays uptake, and rapid nuclear localization was observed (47). Recently, the peptide-based delivery systems of protein transduction domains and cell penetrating peptides, such as human immunodeficiency virus type 1 (HIV-1) Tat-derived protein, have been described (48, 49). It is believed that cell-penetrating Tat peptides exhibit "non-classical import activity" that does not follow the pathways of endocytosis or exocytosis (50); the penetration across the cell membrane and localize in the cytoplasm and nucleus through an energy-independent mechanism and do

not lose their cargo delivery properties when covalently or non-covalently attached to other molecules (51, 52). The peptide-based delivery does not interfere with either specific targeting or hybridization-induced fluorescence of the MBs (53). Tat peptides have received attention as possible vectors for the delivery of hydrophilic drugs and oligonucleotides for gene therapy or other biological applications. This novel delivery method, when combined with nuclease-resistant MBs, could provide a powerful means for rapid detection and real-time monitoring of viral replication in living cells with high specificity and sensitivity.

Several researchers reported that the introduced oligonucleotides via microinjection or with the help of streptolysin O tend to migrate to the nucleus and this nucleus sequestration affects the cytoplasmic target binding (34, 54–56). In contrast, some studies suggest that the MBs delivered into the cells with the help of streptolysin O and cell penetrating peptides reside within the cytoplasm (52, 57). The pathway that these oligodeoxyribonucleotides probes follow for entry into the cell is still unclear and there is no fundamental biological reason why the probes accumulate in the cell nucleus. Ideally, the intracellular delivery should result in a homogenous distribution after probes being introduced into the cells without interfering with either specific targeting or hybridization-induced fluorescence of the probes. The homogenous distribution of probes within the nucleus and cytoplasm will facilitate the study of different viruses with multiple replication and assembly strategies within different cellular compartments in their viral reproductive cycles.

In addition to probing intracellular RNA synthesis during viral replication by the use of MBs, other viral replication events inside a host cell can be exploited for non-invasive detection. In particular, different genetically engineered cell lines have been established to probe this process in a non-invasive manner. Several viral inducible reporter systems have been engineered in the host cell for viral detection based on transcription from viral promoters that are specific for virus-infected cells (58, 59). These transgenic cell lines provide a high level of sensitivity and specificity to facilitate the detection process. Unfortunately, this strategy is not applicable for enteroviruses, which exhibit no defined viral promoter region. Many viruses, such as picornaviruses, retroviruses, and caliciviruses, however, produce a polyprotein that is cleaved into individual proteins by virus-specific proteases (60). Viral protease is a logical target for the detection of infectious viruses because the cleavage event proceeds in a defined manner and is ubiquitous within various viral families. For these viruses, the RNA genome is translated immediately into a single polypeptide upon infection, which is subsequently cleaved by viral proteases to generate mature proteins. This proteolytic process occurs with 100% efficiency and high specificity (61). Furthermore, proteases are diffusible proteins and can act in the *cis* as well as in the *trans* form in the infected cells. This proteolytic step serves as a good candidate for viral detection because these proteases are highly expressed at an early stage of infection and the proteolysis is extremely efficient and selective.

A simple way to monitor this proteolytic event inside a host cell is to engineer a fluorescent protein pair linked by the target peptide sequence of the protease; proteolysis

can be detected based on changes in the fluorescence resonance energy transfer (FRET). FRET is a phenomenon in which energy is transferred from an excited fluorophore, the donor, to a light-absorbing molecule, the acceptor, located within close proximity (typically within 10 nm) (Fig. 1.2) (62). Because of the extreme sensitivity of the efficiency of energy transfer from the donor to the acceptor molecule, high resolution FRET imaging has proven to be a valuable means for studying protein–protein interaction as well as the proteolysis of viral replication in living cells (63, 64). Recently, a FRET reporter cell line expressing a hybrid fluorescent indicator composed of a linker peptide, which is exclusively cleaved by the 2A protease ($2A^{pro}$), flanked with a cyan fluorescent protein (CFP) and a yellow fluorescent protein (YFP) allowed the rapid detection (within 7.5 h) of low numbers of infectious enteroviruses (10 PFU or fewer) (64). In addition, the fluorescence protein pair can be used to probe the dynamic distribution of enterovirus protease in living cells (63). Although most of these analyses have been performed using fluorescence microscopy to evaluate FRET in the areas of interest, flow cytometry has recently been used to provide automated analysis of fluorescent cells for rapid detection of viral infection (65, 66). The success of the above methods is dependent on the development of stable clone expressing the fluorescent substrate for each protease. An alternative is to deliver a synthetic FRET substrate with the linker peptide with specific proteolytic site for each protease into living cell. Successful application of such an approach was reported recently for *in vivo* measurement of cysteine protease calpain (67). FRET substrate for the protease was modified with cell penetrating peptide, heptaarginine at the C-terminal.

While the above *in vivo* techniques demonstrate the real-time monitoring of infectious viruses, the success of these methods requires a living cell system. However, many viruses that cause human gastroenteritis, such as Norwalk virus, adenovirus, and astrovirus, cannot be grown in cell culture or grown poorly. The investigation and development of new cell lines for these epidemiologically important waterborne is a clear first challenge but the urgency cannot be overemphasized as the success in adapting non-culturable viruses to grow in cell culture will allow assessment of the viral replication cycle and the consequent understanding of the biology and epidemiology of these viruses (17). Such knowledge could lead to new strategies for designing and screening drugs against viral infection. Furthermore, real-time molecular detection methods can be combined with the cell culture for rapid detection of infectious viruses and to monitor the progress of viral infection. More sophisticated probes for *in vivo* applications must be able to reduce background in visualizing probe-target hybridization events, to convert target recognition directly into a measurable signal, and to track the multiple steps concerning the production, localization, and transport of specific viral genome during the course of infection.

Recent Development in the Field of Nanotechnology for Viral Detection

MBs and fluorescence protein substrates described above could be readily applied to real-time imaging of gene expression and to study the complexity of viral infection in living cells. A limitation of these molecular probes is the use of organic fluorophore and quencher combinations. The organic fluorophores exhibit low quantum yield and are not suitable for time-lapse microscopy or long-term analysis due to their rapid photobleaching (63, 64). Furthermore, the narrow excitation bands and broad emission bands of the organic dyes cause the spectral overlap and simultaneous light-emission of different probes limit their applications to multiplexing.

Nanotechnology, a field of science that manipulates and utilizes materials on an atomic and molecular scale, generally those less than 100 nm in size, has drawn a growing interest in biological applications for early and specific viral detection (68). Research on inorganic semiconductor nanocrystals, quantum dot (QD), has evolved rapidly on biotechnological and cell-imaging applications. QDs are colloidal particles consisting of a semiconductor core, a high band gap material shell, and typically an outer coating layer. The core-size-dependent photoluminescence (PL) with narrow emission bandwidths that span the visible spectrum and the broad adsorption spectra allow simultaneous excitation of mixed QD populations at a single wavelength. QDs also exhibit several unique features: high quantum yield, high resistance to photodegradation, and better near-infrared (NIR) emission. Research has shown that the brightness and photostability of QDs make single-molecule observation over long time scales possible (69). The simultaneous multicolor approach to single-laser excitation and limited spectral

overlap, which improves sensitivity, makes QD an attractive alternative to conventional methods in biological detection. Simultaneous excitation of several emission-tunable QD populations can be combined with a pool of differentially labeled probes for multiplex target analyses (70–73). The large absorption window of QDs paired with the narrow excitation spectra of acceptor dyes significantly reduces unwanted direct excitation of the acceptor and permits only minimal spectral crosstalk between the donor and acceptor emissions, giving near-zero background (74). These characteristics of QDs in combination with a multicolor flow cytometer were used by Chattopadhyay et al. for studying the phenotype of multiple antigen specific T-cells (75).

Conjugation of QDs with organic quenchers like 4-((4-(dimethylamino)phenyl)azo)benzoic acid (DABCYL) or Iowa Black, brings another issue due to their lower quenching efficiency; especially for dyes emitting at longer wavelengths (76). This may cause problems when different QDs are employed for simultaneous detection of multiple targets. These non-fluorescent quenchers may not absorb energy properly from the excited state of QD thus resulting in higher fluorescence background. Research has shown that the emission of QDs is effectively quenched by contact with gold nanoparticles as a result of DNA hybridization (77). One can envision the potential use of QDs and gold nanoparticles as FRET pairs will improve the detection limits and expand the potential applications of FRET-based molecular probes (78).

References

1. Metcalf, T. G., J. L. Melnick, and M. K. Estes. 1995. Environmental virology: from detection of virus in sewage and water by isolation to identification by molecular biology – a trip of over 50 years. Annu. Rev. Microbiol. 49:461-487.

2. Craun, G. F., R. L. Calderon, and T. J. Wade. 2006. Assessing waterborne risks: an introduction. J. Water and Health 4:3-18.

3. Craun, M. F., G. F. Craun, R. L. Calderon, and M. J. Beach. 2006. Waterborne outbreaks reported in the United States. J. Water and Health 4:19-30.

4. Bosch, A. Human enteric viruses in the water environment: a minireview. 1998. Internatl. Microbiol.1:191-196.

5. Melnick, J. L. Enteric viruses in water. 1984. Monogr. Virol. 15:1-16.

6. Hafliger, D., P. Hubner, and L. Luthy. 2000. Outbreaks of viral gastroenteritis due to sewage-contaminated drinking water. Int. J. Food Microbiol. 54:123-126.

7. Koopmans, M., and E. Duizer. 2000. Foodborne viruses: an emerging problem. 2004. Int. J. Food Microbiol. 90:23-41.

8. Federal Register. 2007. Drinking water: regulatory determinations regarding contaminants on the second drinking water contaminant candidate list - preliminary determinations; proposed rule. 72:24016-24058.

9. Jothikumar, N., T. L. Cromeans, V. R. Hill, X. Lu, M. D. Sobsey, and D. D. Erdman. 2005. Quantitative real-time PCR assays for detection of human adenoviruses and identification of serotypes 40 and 41. Appl. Environ. Microbiol. 71:3131-136.

10. Monpoeho, S., M. Coste-Burel, M. Costa-Mattioli, B. Besse, J. Chomel, S. Billaudel, and V. Ferré. 2002. Application of a real-time polymerase chain reaction with internal positive control for detection and quantification of enterovirus in cerebrospinal fluid. Eur. J. Clin. Microbiol. Infect. Dis. 21:532-536.

11. Stellrecht, K. A., I. Harding, F. M. Hussain, N. G. Mishrik, R. T. Czap, M. L. Lepow, and R. A. Venezia. 2000. A one-step RT-PCR assay using an enzyme-linked detection system for the diagnosis of enterovirus meningitis. J. Clin. Viro. 17:143-149.

12. Valasek, M. A., and J. J. Repa. 2005. The power of real-time PCR. Adv. Physiol. Educ. 29:151–159.

13. Lee, H. K., and Y. S. Jeong. 2004. Comparison of total culturable virus assay and multiplex integrated cell culture-PCR for reliability of waterborne virus detection. Appl. Environ. Microbiol. 70:3632-3636.

14. Euscher, E., J. Davis, I. Holzman, and G. Nuovo. 2001. Coxsackie virus infection of the placenta associated with neurodevelopmental delays in the newborn. Obstet. Gynecol. 98:1019-1026.

15. Morrison, C., T. Gilson, and G. J. Nuovo. 2001. Histologic distribution of fatal rotaviral infection: An immunohistochemical and reverse transcriptase *in situ* polymerase chain reaction analysis. Hum. Pathol. 32:216–221.

16. Wang, D., L. Coscoy, M. Zylberberg, P. C. Avila, H. A. Boushey, D. Ganem, and J. L. DeRisi. 2002. Microarray-based detection and genotyping of viral pathogens. Proc. Natl. Acad. Sci. USA 99:15687-15692.

17. Straub, T. M., K. Höner zu Bentrup, P. Orosz-Coghlan, A. Dohnalkova, B. K. Mayer, R. A. Bartholomew, C. O. Valdez, C. J. Bruckner-Lea, C. P. Gerba, M. Abbaszadegan, and C. A. Nickersont. 2007. *In vitro* cell culture infectivity assay for human noroviruses. Emerg. Infect. Dis. 13:396-403.

18. Bagasra, O. 2007. Protocols for the *in situ* PCR-amplification and detection of mRNA and DNA sequences. Nat. Protoc. 2:2782-2795.

19. Cardoso, T. C., A. C. Rosa, R. D. Astolphi, R. M. Vincente, J. B. Novais, K. Y. Hirata, and M. C. Luvizotto. 2008. Direct detection of infectious bursal disease virus from clinical samples by in situ reverse transcriptase-linked polymerase chain reaction. Avian Pathol. 37:457-461.

20. Nuovo, G. J., P. MacConnell, A. Forde, P. Delvenne. 1991. Detection of human papillomavirus DNA in formalin-fixed tissues by in situ hybridization after amplification by polymerase chain reaction. Am. J. Pathol. 139:847-854.

21. Martin, V., C. Perales, D. Abia, A. R. Ortiz, E. Domingo, C. Briones. 2006. Microarray-based identification of antigenic variants of foot-and-mouth disease virus: a bioinformatics quality assessment. BMC Genomics 7; No pp. given.

22. Gyarmati, P., T. Conze, S. Zohari, N. LeBlanc, M. Nilsson, U. Landegren, J. Banér, and S. Belák. 2008. Simultaneous genotyping of all hemagglutinin and neuraminidase subtypes of avian influenza viruses by use of padlock probes. J. Clin. Microbiol. 46:1747-1751.

23. Jabado, O. J., Y. Liu, S. Conlan, P. L. Quan, H. Hegyi, Y. Lussier, T. Briese, G. Palacios, and W. I. Lipkin. 2008. Comprehensive viral oligonucleotide probe design using conserved protein regions. Nucleic Acids Res. 36:e3.

24. Chapron, C. D., N. A. Ballester, J. H. Fontaine, C. N. Frades, and A. B. Margolin. 2000. Detection of astroviruses, enteroviruses, and adenovirus types 40 and 41 in surface waters collected and evaluated by the information collection rule and an integrated cell culture-nested PCR procedure. Appl. Environ. Microbiol. 66:2520-2525.

25. Cromeans, T., M. D. Sobsey, and H. A. Fields. 1987. Development of a plaque assay for a cytopathic, rapidly replicating isolate of hepatitis A virus. J. Med. Virol. 22:45-56.

26. Nainan, O. V., G. Xia, G. Vaughan, and H. S. Margolis. 2006. Diagnosis of hepatitis A virus infection: a molecular approach. Clin. Microbiol. Rev. 19:63-79.

27. Dotzauer, A., U. Gebhardt, K. Bieback, U. Göttke, A. Kracke, J. Mages, S. M. Lemon, and A. Vallbracht. 2000. Hepatitis A virus-specific immunoglobulin A mediates infection of hepatocytes with hepatitis A virus via the asialoglycoprotein receptor. J. Virol. 74:10950-10957.

28. Tyagi, S., and F. R. Kramer. 1996. Molecular beacons: probes that fluoresce upon hybridization. Nat. Biotech. 14:303-308.

29. Drake, T. J., and W. Tan. 2004. Molecular beacon DNA probes and their bioanalytical applications. Applied Spectroscopy 58:269-280.

30. Fang, X., J. J. Li, J. Perlette, W. Tan, and K. Wang. 2000. Molecular beacons: novel fluorescent probes. Anal. Chem. 72:747A-753A.

31. Goel, G., A. Kumar, A. K. Puniya, W. Chen, and K. Singh. 2005. Molecular beacon: a multitask probe. J. Appl. Microbiol. 99:435-442.

32. Marras, S. A. E, F. R. Kramer, and S. Tyagi. 1999. Multiplex detection of single-nucleotide variations using molecular beacons. Genet. Anal-Bionol. E. 14:151-156.

33. Tyagi, S., D. P. Bratu, and F. R. Kramer. 1997. Multicolor molecular beacons for allele discrimination. Nat. Biotech. 16:49-53.

34. Tyagi, S., and O. Alsmadi. 2004. Imaging Native β-Actin mRNA in Motile Fibroblasts. Biophys. J. 87:4153–4162.

35. Galil, K. H. A. E., M. A. E. Sokkary, S. M. Kheira, A. M. Salazar, M. V. Yates, W. Chen, and A. Mulchandani. 2004. Combined immunomagnetic separation-molecular beacon-reverse transcription-PCR assay for detection of hepatitis A virus from environmental samples. Appl. Environ. Microbiol. 70:4371-4374.

36. Wang, A., A. M. Salazar, M. V. Yates, A. Mulchandani, and W. Chen. 2005. Visualization and detection of infectious coxsackievirus replication using a combined cell culture-molecular beacon assay. Appl. Environ. Microbiol. 71:8397-8401.

37. Yeh, H. Y., Y. C. Hwang, M. V. Yates, A. Mulchandani, and W. Chen. 2008. Detection of hepatitis A virus by using a combined cell Culture-molecular beacon assay. Appl. Environ. Microbiol. 74:2239-2243.

38. Cui, Z. Q., Z. P. Zhang, X. E. Zhang, J. K. Wen, Y. F. Zhou, and W. H. Xie. 2005. Visualizing the dynamic behavior of poliovirus plus-strand RNA in living host cells. Nucleic Acids Res. 33:3245–3252.

39. Dirks, R. W., C. Molenaar, and H. J. Tanke. 2001. Methods for visualizing RNA processing and transport pathways in living cells. Histochem. Cell Biol. 115:3–11.

40. Li, J. J., R. Geyer, and W. Tan. 2000. Using molecular beacons as a sensitive fluorescence assay for enzymatic cleavage of single-stranded DNA. Nucleic Acids Res. 28:e52.

41. Bratu, D. P., B.-J. Cha, M. M. Mhlanga, F. R. Kramer, and S. Tyagi. 2003. Visualizing the distribution and transport of mRNAs in living cells. Proc. Natl. Acad. Sci. USA 100:13308–13313.

42. Cotten, M., B. Oberhauser, H. Brunar, A. Holzner, G. Issakides, C. R. Noe, G. Schaffner, E. Wagner, and M. L. Birnstiel. 1991. 2'-O-methyl, 2'-O-ethyl oligoribonucleotides and phosphorothioate oligodeoxyribonucleotides as inhibitors of the in vitro U7 snRNP-dependent mRNA processing event. Nucleic Acids Res. 19:2629–2635.

43. Fisher, T. L., T. Terhorst, X. Cao, and R. W. Wagner. 1993. Intracellular disposition and metabolism of fluorescently-labeled unmodified and modified oligonucleotides microinjected into mammalian cells. Nucleic Acids Res. 21:3857-3865.

44. Molenaar, C., S. A. Marras, J. C. M. Slats, J. C. Truffert, M. Lemaitre, A. K. Raap, R. W. Dirks, and H. J. Tanke. 2001. Linear 2' O-Methyl RNA probes for the visualization of RNA in living cell. Nucleic Acids Res. 29:e89.

45. Tsourkas, A., M. A. Behlke, and G. Bao. 2002. Hybridization of 2’-O-methyl and 2’-deoxy molecular beacons to RNA and DNA targets. Nucleic Acids Res. 30:5168-5174.

46. Santangelo, P. J., N. Nitin, L. LaConte, A. Woolums, and G. Bao. 2006. Live-cell characterization and analysis of a clinical isolate of bovine respiratory syncytial virus, using molecular beacons. J. Virol. 80:682–688.

47. Spiller, D. G., R. V. Giles, J. Grzybowski, D. M. Tidd, and R. E. Clark. 1998.

Improving the intracellular delivery and molecular efficacy of antisense oligonucleotides in chronic myeloid leukemia cells: a comparison of streptolysin-O permeabilization, electroporation, and lipophilic conjugation. Blood 91:4738-4746.

48. Deshayes, S., M. C. Morris, G. Divita, and F. Heitz. 2005. Cell-penetrating peptides: tools for intracellular delivery of therapeutics. Cell Mol. Life Sci. 62:1839-1849.

49. Wadia, J. S., and S. F. Dowdy. 2002. Protein transduction technology. Curr. Opin. Biotechnol. 13:52-56.

50. Kueltzo, L. A., and C. R. Middaugh. 2003. Nonclassical transport proteins and peptides: An alternative to classical macromolecule delivery systems. J. Pharm. Sci. 92:1754-1772.

51. Kueltzo, L. A., and C. R. Middaugh. 2000. Potential use of non-classical pathways for the transport of macromolecular drugs. Expert Opinion on Investigational Drugs 9:2039-2050.

52. Saalik, P., A. Elmquist, M. Hansen, K. Padari, K. Saar, K. Viht, U. Langel, and M. Pooga. 2004. Protein cargo delivery properties of cell-penetrating peptides. A comparative study. Bioconjugate Chem. 15:1246-1253.

53. Nitin, N., P. J. Santangelo, G. Kim, S. Nie, and G. Bao. 2004. Peptide-linked molecular beacons for efficient delivery and rapid mRNA detection in living cells. Nucleic Acids Res. 32:e58.

54. Chen, A. K., M. A. Behlke, and A. Tsourkas. 2007. Avoiding false-positive signals with nuclease-vulnerable molecular beacons in single living cells. Nucleic Acids Res. 35:e105.

55. Mhlanga, M. M., D. Y. Vargas, C. W. Fung, F. R. Kramer, and S. Tyagi. 2005. tRNA-linked molecular beacons for imaging mRNAs in the cytoplasm of living cells. Nucleic Acids Res. 33:1902-1912.

56. Tsuji, A., H. Koshimoto, Y. Sato, M. Hirano, Y. Sei-Iida, S. Kondo, and K. Ishibashi. 2000. Direct observation of specific messenger RNA in a single living cell under a fluorescence microscope. Biophys. J. 78:3260–3274.

57. Watzinger, F., K. Ebner, and T. Lion. 2006. Detection and monitoring of virus infections by real-time PCR. Mol. Aspects Med. 254-298.

58. Olivo, P. D. 1996. Transgenic cell lines for detection of animal viruses. Clin. Microbiol. Rev. 9:321-334.

59. Rider, T. H., M. S. Petrovick, F. E. Nargi, J. D. Harper, E. D. Schwoebel, R. H. Mathews, D. J. Blanchard, L. T. Bortolin, A. M. Young, J. Chen, and M. A. Hollis. 2003. A B cell-based sensor for rapid identification of pathogens. Science 301:213-215.

60. Strauss, J. H. 1990. Semin. Virol. 1:307-384.

61. Alvey, J. C., E. E. Wyckoff, S. F. Yu, R. Lloyd, and E. Ehrenfeld. 1991. *cis*- and *trans*-cleavage activities of poliovirus 2A protease expressed in Escherichia coli. J. Virol. 65:6077-6083.

62. Jares-Erijman, E. A., and T. M. Jovin. 2003. FRET imaging. Nat. Biotechnol 21:1387-1395.

63. Hsu, Y. Y., Y. N. Liu, W. Wang, F. J. Kao, and S. H. Kung. 2007. *In vivo* dynamics of enterovirus protease revealed by fluorescence resonance emission transfer (FRET) based on a novel FRET pair. Biochem. Biophys. Res. Commun. 353:939-945.

64. Hwang, Y. C., W. Chen, and M. V. Yates. 2006. Use of fluorescence resonance energy transfer for rapid detection of enteroviral infection *in vivo*. Appl. Environ. Microbiol. 72:3710-3715.

65. Bolton, D. L., and M. J. Lenardo. 2007. Vpr cytopathicity independent of G2/M cell cycle arrest in human immunodeficiency virus type 1-infected CD4+ T cells. J. Virol. 81:8878-8890.

66. Niapour, M., and S. Berger. 2007. Flow cytometric measurement of calpain activity in living cells. Cytometry A 71:475-485.

67. Bánóczi, Z., A. Alexa, A. Farkas, P. Friedrich, and F. Hudecz. 2008. Novel cell-penetrating calpain substrate. Bioconjug. Chem. 19:1375-1381.

68. Bentzen, E., D. W. Wright, and J. E. Crowe Jr. 2006. Nanoscale tools for rapid and sensitive diagnosis of viruses. Future Virol. 1:769-781.

69. Michalet, X., F. F. Pinaud, L. A. Bentolila, J. M. Tsay, S. Doose, J. J. Li, G. Sundaresan, A. M. Wu, S. S. Gambhir, and S. Weiss. 2005. Quantum dots for live cells, *in vivo* imaging, and diagnostics. Science. 307:538-544.

70. Mattoussi, H., J. M. Mauro, E. R. Goldman, G. P. Anderson, V. C. Sundar, F. V. Mikulec, and M. G. Bawendi. 2000. Self-assembly of CdSe-ZnS quantum dot bioconjugates using an engineered recombinant protein. J. Am. Chem. Soc. 122:12142-12150.

71. Medintz, I. L., A. R. Clapp, H. Mattoussi, E. R. Goldman, B. Fisher, and J. M. Mauro. 2003. Self-assembled nanoscale biosensors based on quantum dot FRET donors. Nature Materials 2:630-638.

72. Medintz, I. L., J. H. Konnert, A. R. Clapp, I. Stanish, M. E. Twigg, H. Mattoussi, J. M. Mauro, J. R. Deschamps. 2004. A fluorescence resonance energy transfer-derived structure of a quantum dot-protein bioconjugate nanoassembly. Proc. Natl. Acad. Sci. USA 101:9612-9617.

73. Zhang, C-Y., H-C. Yeh, M. T. Kuroki, and T-H. Wang. 2005. Single-quantum-dot-based DNA nanosensor. Nature Materials. 4:826-831.

74. Clapp, A. R., I. L. Medintz, J. M. Mauro, B. R. Fisher, M. G. Bawendi, and H. Mattoussi. 2004. Fluorescence resonance energy transfer between quantum dot donors and dye-labeled protein acceptors. J. Am. Chem. Soc. 126:301-310.

75. Chattopadhyay, P. K., D. A. Price, T. F. Harper, M. R. Betts, J. Yu, E. Gostick, S. P. Perfetto, P. Goepfert, R. A. Koup, S. C. De Rosa, M. P. Bruchez, and M. Roederer.2006. Quantum dot semiconductor nanocrystals for immunophenotyping by polychromatic flow cytometry. Nat. Med. 12:972-977.

76. Dubertret, D., M. Calame, and A. J. Libchaber. 2001. Single-mismatch detection using gold-quenched fluorescent oligonucleotides. Nat. Biotechnol. 19:365-370.

77. Dyadyusha, L., H. Yin, S. Jaiswal, T. Brown, J. J. Baumberg, F. P. Booy, and T. Melvin. 2005. Quenching of CdSe quantum dot emission, a new approach for biosensing. Chem. Commun. 25:3201-3203.

78. Wargnier, R., A. V. Baranov, V. G. Maslov, V. Stsiapura, M. Artemyev, M. Pluot, A. Sukhanova, and I. Nabiev. 2004. Energy transfer in aqueous solutions of oppositely charged CdSe/ZnS core/shell quantum dots and in quantum dot-nanogold assemblies. Nano Lett. 4:451-457.

Legends to Figures

Fig. 1.1. MBs report the presence of picornavirus by visualizing the fluorescent hybrids with viral RNAs under the fluorescence microscope during the course of viral reproduction, such as: (A) uncoating of viral genome, (B) RNA translation associated with ribosomes (gray) and (C) RNA synthesis on the surface of infected-cell-specific membrane vesicles.

Fig. 1.2. Schematic representation of fluorescent indicator for monitoring viral proteolytic processing in the infected cells. Detection of infectious viruses will be indicated by changes in FRET (modified from Ref. 64).

Fig. 1.1.

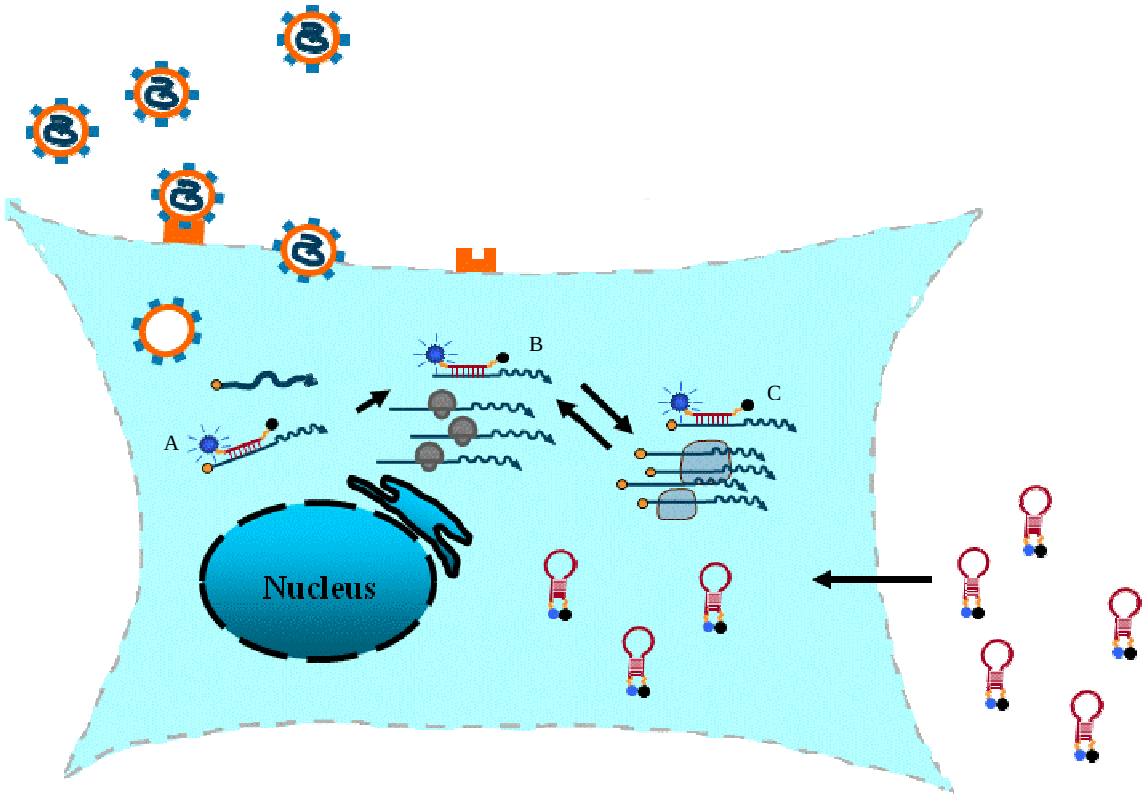

Fig. 1.2.

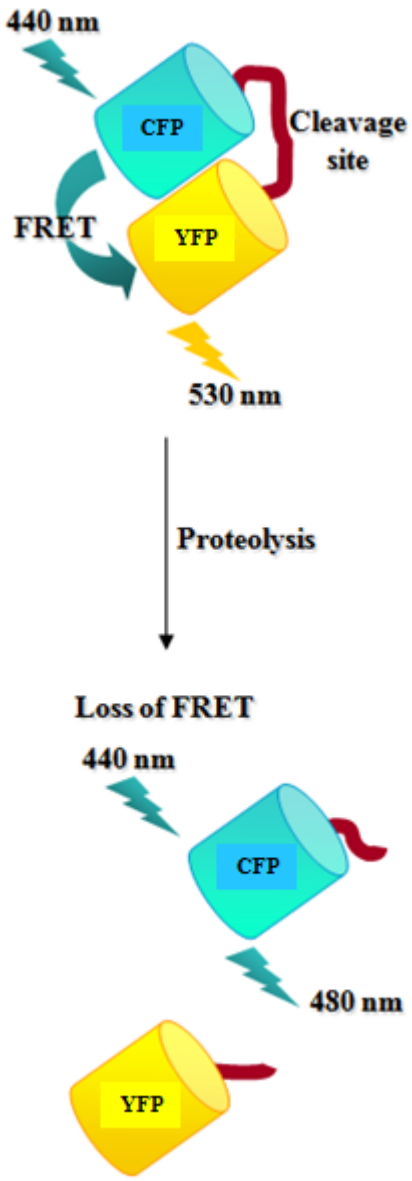
440 nm
CFP
Cleavage site
FRET
YFP
530 nm
Proteolysis
Loss of FRET
440 nm
CFP
480 nm
YFP

Chapter 2:

Detection of hepatitis A virus by using a combined cell-culture – molecular beacon assay

Abstract

Rapid and efficient methods for the detection and quantification of infectious viruses are required for public health risk assessment. Current methods to detect infectious viruses are based on mammalian cell culture and rely on the production of visible cytopathic effects (CPE). For hepatitis A virus (HAV), viral replication in cell culture has been reported to be nonlytic and relatively slow. It may take more than 1 week to reach the maximum production and subsequent visualization of CPE. A molecular beacon (MB), H1, specifically targeting a 20-bp 5' noncoding region of HAV, was designed and synthesized. MB H1 was introduced into fixed and permeabilized fetal rhesus monkey kidney (FRhK-4) cells infected with HAV strain HM-175. Upon hybridizing with the viral mRNA, fluorescent cells were visualized easily under a fluorescence microscope. Discernible fluorescence was detected only in infected cells by using the specific MB H1. A nonspecific MB, which was not complementary to the viral RNA sequence, produced no visible fluorescence signal. This MB-based fluorescence assay enabled the direct counting of fluorescent cells and could achieve a detection limit of 1 PFU at 6 h postinfection (p.i.), demonstrating a significant improvement in viral quantification over current infectivity assays.

Introduction

Hepatitis A virus (HAV), a positive single-stranded RNA virus, was previously classified as enterovirus type 72 (1) and has now been classified in the *Hepatovirus* genus of the *Picornaviridae* family (2). These single-plus-stranded RNA viruses can directly translate plus-strand RNA genomes into protein using the host ribosomes. The plus strand is transported to the infected cell via specific membrane vesicles, where it is copied into full-length minus strands. These minus strands then serve as templates for the synthesis of plus-strand genomic RNA molecules (3, 4).

HAV is known to cause acute liver infection with a discrete onset of symptoms (e.g., fever, malaise, and nausea), followed in several days by jaundice. Person-to-person transmission through the fecal-oral route is the primary means of HAV transmission. Outbreaks and periodic cases also occur from exposure to fecally contaminated food or water (Centers for Disease Control and Prevention). Most picornaviruses are lytic, causing distinctive cytopathic effects and replicating in an 8-h cycle under one-step growth conditions. The growth of HAV in cell culture systems, however, is much slower and nonlytic and does not produce a detectable cytopathic effect in infected cells (5). Cromeans et al. reported the isolation of a cytopathic HAV variant from the rapidly replicating isolate HM-175 that is lytic for fetal rhesus monkey kidney (FRhK-4) cells (6). However, complete lysis still did not occur until 5 to 6 days postinfection (p.i.).

Conventional methods for detecting infectious HAV rely on viral propagation in cell culture, radioimmunoassay, immunofluorescenceor, plaque assay; these methods are difficult to perform, and it may take weeks before the viruses reach sufficiently high

amounts in the cell-culture medium to allow detection (6-9). For public health assessments, this long delay in obtaining infectivity information may affect the process of epidemic control strategies. Improved methods need to be developed for the rapid and reliable detection and quantification of infectious viruses.

Molecular beacons (MBs) were first developed in 1996 (10) and have been applied in numerous in vitro hybridization assays (11-13). MBs are single-stranded oligonucleotide probes possessing stem-loop structures and are doubly labeled with a fluorophore and a quencher at the 5' and 3' ends, respectively.

In the presence of a complementary sequence, the MB undergoes a conformational change and the MB fluoresces via fluorescence resonance energy transfer. Because of this property, MBs provide a separation-free detection scheme that produces fluorescence upon binding to the targets. MBs have been widely used in many areas, such as in real-time monitoring of DNA/RNA amplification during PCR, gene typing, mutation detection, real-time enzymatic cleavage assay (12, 14), and RNA detection in living cells (15, 16). By probing the endogenous RNA with MBs, the dynamic behavior of poliovirus plus-strand RNA in living host cells has been studied (16). The use of MBs as a rapid and sensitive tool to detect and quantify the presence of newly synthesized coxsackievirus RNA has also been demonstrated (17).

This report demonstrates a combined cell culture-MB assay for the detection of infectious HAV with a detection limit of 1 PFU within 6 h p.i. Validation of this MB-based fluorescence assay for viral quantification was demonstrated, with results

compatible with those of the conventional plaque assay. Finally, the utility of the assay for the detection of HAV in surface water samples was also demonstrated.

Materials and Methods

FRhK-4 cell culture.

FRhK-4 cells (ATCC CRL-1688; passage level of < 40) were grown in 400 mL 1X autoclavable minimal essential medium (Irvine Scientific, Santa Ana, CA) with 4 mL 7.5% sodium bicarbonate, 8 mL 1 M Hepes, 4 mL nonessential amino acids (Gibco BRL, Grand Island, NY), 10 mL A/B-L (1,000 U/mL penicillin, 1,000 U/mL streptomycin, 2 mg/mL kanamycin, 2,000 U/mL nystatin, and 80 mM L-glutamine), and 60 mL fetal bovine serum (Sigma-Aldrich, St. Louise, MO) at 37°C in a 5% CO_2 atmosphere. Phosphate-buffered saline (PBS; 0.01 M phosphate, pH 7.4, 0.138 M NaCl, and 2.7 mM KCl) and Trisbuffered saline solution (TBSS; 0.05 M Tris, pH 7.4, 0.28 M NaCl, 10 mM KCl, and 0.82 mM Na_2HPO_4) were used for washing steps in the plaque assay and MB analysis, respectively.

Virus preparation.

The cytopathic HM-175 strain of HAV (ATCC VR-2089) was inoculated into uninfected FRhK-4 cells (passage numbers 34 to 36) for 7 days at 37°C in a 5% CO_2 atmosphere. The cell lysate was purified (-20°C freezing and 37°C thawing by turns) and then extracted with chloroform. The HM-175 virus stock was stored at -80°C.

Plaque assay.

The HM-175 virus stock was thawed, and then a 10-fold serial dilution in PBS was performed. Confluent, 7-day-old FRhK-4 monolayers in 24-well, 15-mm dishes (Costar; Corning Inc., Corning, NY) were infected with 0.5 mL of virus dilutions. After 90 min of adsorption at 37°C in 5% CO_2, the solutions were aspirated and the monolayers were washed once with PBS. One milliliter of 100-mL 2% carboxymethylcellulose sodium salt (Sigma-Aldrich, St. Louis, MO) in 100 mL 2X autoclavable minimal essential medium (Irvine Scientific, Santa Ana, CA) with 2 mL 7.5% sodium bicarbonate, 4 mL 1 M Hepes, 2 mL nonessential amino acids, 5 mL A/B-L (1,000 U/mL penicillin, 1,000 U/mL streptomycin, 2 mg/mL kanamycin, 2,000 U/mL nystatin, and 80 mM L-glutamine), and 30 mL fetal bovine serum (Sigma-Aldrich, St. Louis, MO) was added. After 8 days of incubation at 37°C in 5% CO_2, the carboxymethylcellulose overlay was removed and the cells were washed once with PBS. One milliliter 0.8% crystal violet/3.7% formaldehyde solution was added, and the plate was returned to the 37°C incubator for overnight incubation before counting. Excess stain was removed by washing with de-ionized water, and plaques were enumerated.

MB design.

The design of MB H1 was based on an alignment of the sequences of 26 different HAV strains obtained from GenBank. The DNA folding program mfold (www.bioinfo.rpi.edu/applications/mfold/dna/) and IDT SciTools (www.idtdna.com/SciTools/SciTools.aspx) were used to predict the thermodynamic

properties and the secondary structures of MBs. MB H1 (5'-6-carboxyfluorescein-CTTGGGCCGCCGCTGTTACCCTATCCCCCAAG-DABCYL-3' [the stem sequence is underlined]) was designed to be specifically hybridized to a 20-bp region (421 to 480 bp of the genome) of the 5' untranslated region of HAV genomic RNA. The thermal denaturation profile was determined on an iCycler iQ multicolor real-time PCR detection system (Bio-Rad, Hercules, CA) by monitoring the fluorescence of a 50-μL volume of a solution containing 5 μM MB H1 dissolved in 100 mM Tris-HCl (pH 8.0) containing 1 mM $MgCl_2$ as the temperature was decreased from 90°C to 10°C at a rate of 1°C/min. The fluorescence of 50 μL of a solution of 5 μM MB H1/oligonucleotide hybrids was also monitored for comparison. The probe 5'-6-carboxyfluorescein-CGCTATGCATCCGGTCAGTGGCAGTATAGCG-DABCYL-3' was used for the nonspecific MB study.

Fixation, permeabilization, and incubation.

FRhK-4 cells were cultured to confluence in eight-well Lab-Tek II CC2 chamber slides (Fisher Scientific, NJ) at 37°C in 5% CO_2. After incubation for predetermined time periods, the slides were removed from the 37°C incubator. The medium was aspirated, and the cells were washed twice with TBSS. The cells were fixed with 2% (wt/vol) paraformaldehyde in TBSS for 20 min at room temperature, washed three times with TBSS, and then permeabilized with 0.1% Triton X-100 in TBSS for 5 min at 4°C. Following three washes with TBSS, the cells were incubated with 5 μM MB H1 for 1 h at

room temperature in the dark. Later, the slides were washed twice with TBSS and observed under a fluorescence microscope with the chambers containing TBSS.

Fluorescence microscopy and image processing.

The optical setup for fluorescence imaging consisted of a BX51 fluorescence microscope, a 100W Osram mercury burner, filter wheels for excitation filters, emission filters, dichroic mirrors, a 10X/0.30 objective lens and a QImaging Retiga EXI monochrome camera (Olympus America, Inc., San Diego, CA). Both phase-contrast and fluorescent images were taken and analyzed using Image-Pro Plus (Media Cybernetics, Inc., Bethesda, MD).

Enumeration of fluorescent cells.

A magnification of 100X (10X objective and 10X eyepiece) was used for observing fluorescent cells. For each 0.7-cm^2 glass chamber well, approximately 117 fields could be visualized at a magnification of 100X. To calculate the value for infected cells in each chamber well, both phase-contrast (to count the total number of cells) and fluorescent (to count the number of infected cells) images of 30 randomly chosen areas were taken at a magnification of 100X. The number of fluorescent cells within the chosen area was recorded by Image-Pro Plus software.

Results and Discussion

Visualization of infected FRhK-4 cells using MBs.

MB H1 was designed to target a 20-bp common sequence of the 5' untranslated region of 26 different HAV strains. In our previous study (17), fixation and permeabilization were used to introduce MBs into BGMK cells. To test whether the same procedure would work with FRhK-4 cells, MB H1/oligonucleotide hybrids were first introduced into uninfected cells. After 1 h of incubation, 100% of cells were brightly fluorescent, indicating that the same procedure works well even with FRhK-4 cells (Fig. 2.1, panels III). Next, the ability to detect HAV viral RNA was tested by introducing MB H1 into highly infected cells (10^5 PFU for 24 h) and uninfected cells. As expected, 100% of the highly infected cells were brightly fluorescent (Fig. 2.1, panels IV), while only background fluorescence was observed for the uninfected cells (Fig. 2.1, panels I). These results confirm that the MBs specifically recognize the HAV RNA. In addition, the introduction of a nonspecific MB that is not complementary to the HAV RNA produced a negligible amount of fluorescence (Fig. 2.1, panels II), demonstrating the specificity of the reported method.

Visualization of HAV replication.

To investigate whether this approach can be used to rapidly detect low doses of infectious HAV, cultures infected with 1 PFU of HAV were analyzed from 6 to 48 h p.i. in order to investigate the minimum time required to consistently detect a positive fluorescent signal. As shown in Fig. 2.2, fluorescent cells can be visualized within 6 h p.i. and the number of

fluorescent cells increased with increasing infection times. The average number of fluorescent cells at different p.i. time points was calculated by direct counting using a fluorescence microscope at 100X magnification to provide a better quantitative assessment. A significantly higher number of fluorescent cells (~50) was detected for the infected cultures at 6 h p.i. than for the uninfected cultures (0 PFU), where roughly 20 fluorescent cells were detected independently of infection time (Fig. 2.3). The number of fluorescent cells increased rapidly from 50 to 90 from 6 to 12 h p.i. and remained relatively constant thereafter. This result is indicative of the fairly slow replication process for HAV, suggesting that a complete lytic cycle may take more than 48 h, consistent with previous reports (6-9). Unlike the long lytic cycle, less than 6 h was required to detect the synthesis of HAV RNA, enabling the rapid detection of infectious HAV.

Quantification of infectious HAV dosages.

To investigate whether this 6-h infection window could be used to quantify infectious HAV, cells were infected with 1 to 200 PFU HAV and the average number of fluorescent cells was recorded. A linear correlation was obtained by plotting the number of fluorescent cells versus the number of PFU (Fig. 2.4), indicating that this MB-based fluorescence assay can be used as a quantification tool for detecting infectious HAV. The number of PFU can be calculated easily by using the correlation obtained after direct counting of fluorescent cells. More importantly, the method can be used to provide the

rapid quantification of infectious HAV doses within 6 h p.i. compared to that with the 8-day incubation period for the conventional plaque assay.

Detection of HAV in environmental water samples and comparison with plaque assay.

Using the 6-h infection window, the utility of the MB-based fluorescence assay for environmental samples was tested by using runoff water samples collected from Davis, CA, spiked with HAV. FRhK-4 cells were incubated with water samples spiked with different amounts of HAV, and the resulting infectious doses were determined based on the calibration curve shown in Fig. 2.4. In parallel, the conventional 8-day plaque assay was carried out to determine the infectious doses. The infectious dosages obtained from the two assays were remarkably similar (Fig. 2.5, table inset), with a maximum of 25% difference, validating the utility of the assay for viral quantification in real water samples.

In conclusion, the reported fluorescence assay combines a 32-fold reduction in detection time with a quantitative capability similar to that for the 8-day conventional plaque assay. The reported MB-based fluorescence assay is particularly attractive for environmental viral quantification, which focuses particularly on the lower infectious doses.

References

1. Melnick, J. L. 1982. Classification of hepatitis A virus as enterovirus type 72 and of hepatitis B virus as hepadnavirus type 1. Intervirology 18:105–106.

2. Minor, P. D., F. Brown, E. Domingo, E. Hoey, A. King, N. Knowles, S. Lemon, A. Palmenberg, R. R. Rueckert, G. Stanway, E. Wimmer, and M. Yin-Murphy. 1995. Family Picornaviridae. In F. A. Murphy, C. M. Fauquet, D. H. L. Bishop, S. A. Ghabrial, A. W. Jarvis, G. P. Martelli, M. A. Mayo, and M. D. Summers (ed.), Virus taxonomy. Sixth report of the International Committee for the Taxonomy of Viruses. Springer-Verlag, New York, NY.

3. Andino, R., N. Boddeker, and A. V. Gamarnik. 1999. Intracellular determinants of picornavirus replication. Trends Microbiol. 7:76–82.

4. Baltimore, D. 1971. Expression of animal virus genomes. Bacteriol. Rev. 35:235–241.

5. Koch, F., and G. Koch. 1985. The molecular biology of poliovirus. Springer-Verlag, New York, NY.

6. Cromeans, T., M. D. Sobsey, and H. A. Fields. 1987. Development of a plaque assay for a cytopathic, rapidly replicating isolate of hepatitis A virus. J. Med. Virol. 22:45–56.

7. Cromeans, T., H. A. Fields, and M. D. Sobsey. 1989. Replication kinetics and cytopathic effect of hepatitis A virus. J. Gen. Virol. 70:2051–2062.

8. Flehmig, B. 1980. Hepatitis A virus in cell culture. I. Propagation of different hepatitis A virus isolates in a fetal rhesus monkey kidney cell line (FRhK-4). Med. Microbiol. Immunol. 168:239–248.

9. Flehmig, B. 1981. Hepatitis A virus in cell culture. II. Growth characteristics of hepatitis A virus in FRhK-4/R cells. Med. Microbiol. Immunol. 170:73–81.

10. Tyagi, S., and F. R. Kramer. 1996. Molecular beacons: probes that fluoresce upon hybridization. Nat. Biotechnol. 14:303–308.

11. Drake, T. J., and W. Tan. 2004. Molecular beacon DNA probes and their bioanalytical applications. Appl. Spectrosc. 58:269–280.

12. Fang, X., J. J. Li, J. Perlette, W. Tan, and K. Wang. 2000. Molecular beacons: novel fluorescent probes. Anal. Chem. 72:747A–753A.

13. Goel, G., A. Kumar, A. K. Puniya, W. Chen, and K. Singh. 2005. Molecular beacon: a multitask probe. J. Appl. Microbiol. 99:435–442.

14. Galil, K. H. A. E., M. A. E. Sokkary, S. M. Kheira, A. M. Salazar, M. V. Yates, W. Chen, and A. Mulchandani. 2004. Combined immunomagnetic separation–molecular beacon–reverse transcription-PCR assay for detection of hepatitis A virus from environmental samples. Appl. Environ. Microbiol. 70:4371–4374.

15. Bratu, D. P., B.-J. Cha, M. M. Mhlanga, F. R. Kramer, and S. Tyagi. 2003. Visualizing the distribution and transport of mRNAs in living cells. Proc. Natl. Acad. Sci. USA 100:13308–13313.

16. Cui, Z. Q., Z. P. Zhang, X. E. Zhang, J. K. Wen, Y. F. Zhou, and W. H. Xie. 2005. Visualizing the dynamic behavior of poliovirus plus-strand RNA in living host cells. Nucleic Acids Res. 33:3245–3252.

17. Wang, A., A. M. Salazar, M. V. Yates, A. Mulchandani, and W. Chen. 2005. Visualization and detection of infectious coxsackievirus replication using a combined cell culture-molecular beacon assay. Appl. Environ. Microbiol. 71:8397–8401.

Legends to Figures

Fig. 2.1. Visualization of uninfected or infected FRhK-4 cells by introducing MBs. Cells were fixed and permeabilized before 1 h of incubation with 5 µM MB. (Panels I) Uninfected cells with MB H1. (Panels II) Highly infected (10^5 PFU) FRhK-4 cells at 24 h p.i. with a nonspecific MB. (Panels III) Uninfected cells with MB H1/oligonucleotide hybrids. (Panels IV) Highly infected (10^5 PFU) FRhK-4 cells at 24 h p.i. with MB H1. Scale bar, 20 µm.

Fig. 2.2. Visualization of FRhK-4 cells infected with 1 PFU at various p.i. time points. Cells infected with 1 PFU were fixed and permeabilized before 1 h of incubation with 5 µM MB H1. Scale bar, 20 µm.

Fig. 2.3. The numbers of fluorescent cells at different p.i. time points. FRhK-4 cells infected with 0 or 1 PFU for 6, 12, 18, 24, and 48 h p.i. were fixed and permeabilized before 1 h of incubation with 5 µM MB H1. The number of fluorescent cells was counted using a fluorescence microscope at 100X magnification. Error bars represent the standard deviations for three replicates.

Fig. 2.4. The correlation between the number of fluorescent cells and the number of PFU at 6 h p.i. The fluorescent images from 30 different fields within a chosen chamber well were captured under a fluorescence microscope at 100X magnification. The numbers of fluorescent cells were recorded and averaged. The 8-day plaque assay was performed to

confirm the average infectious doses. Error bars represent the standard deviations for three replicates.

Fig. 2.5. Comparison of infectious HAV doses determined by the conventional 8-day plaque assay and the MB-based fluorescence assay. FRhK-4 cells infected with unknown viral doses for 6 h were fixed and permeabilized before 1 h of incubation with 5 μM MB H1. The number of fluorescent cells from 30 different fields within a chosen chamber well was recorded, and the PFU value was calculated based on the calibration equation from Fig. 2.4. In parallel, the infectious viral doses were determined independently by using the 8-day plaque assay. Error bars represent the standard deviations (SD) for three replicate experiments. The inset shows the infectivity data obtained from two assays.

Fig. 2.1.

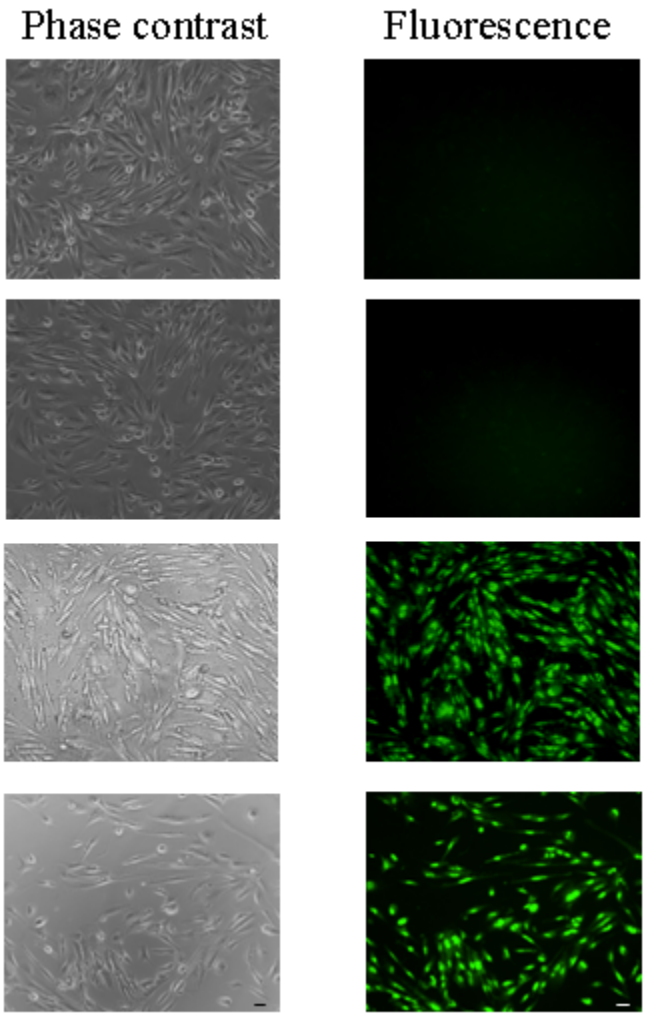

Fig. 2.2.

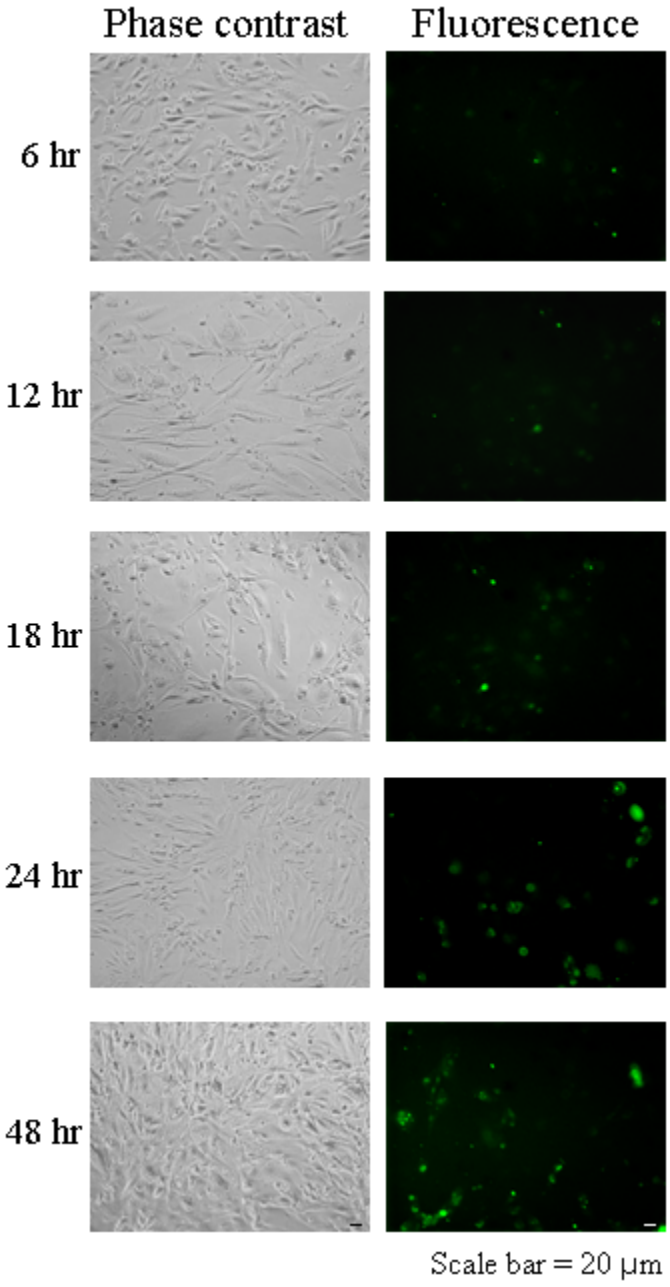
Phase contrast
Fluorescence
6 hr
12 hr
18 hr
24 hr
48 hr
Scale bar = 20 μm

Fig. 2.3.

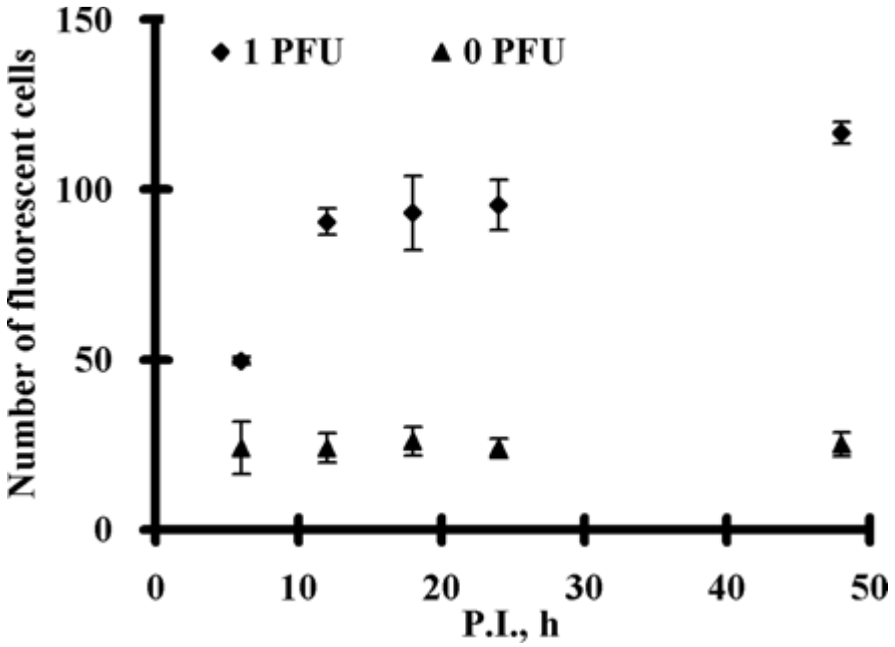
150
100
50
0
Number of fluorescent cells
◆ 1 PFU
▲ 0 PFU
0
10
20
30
40
50
P.I., h

Fig. 2.4.

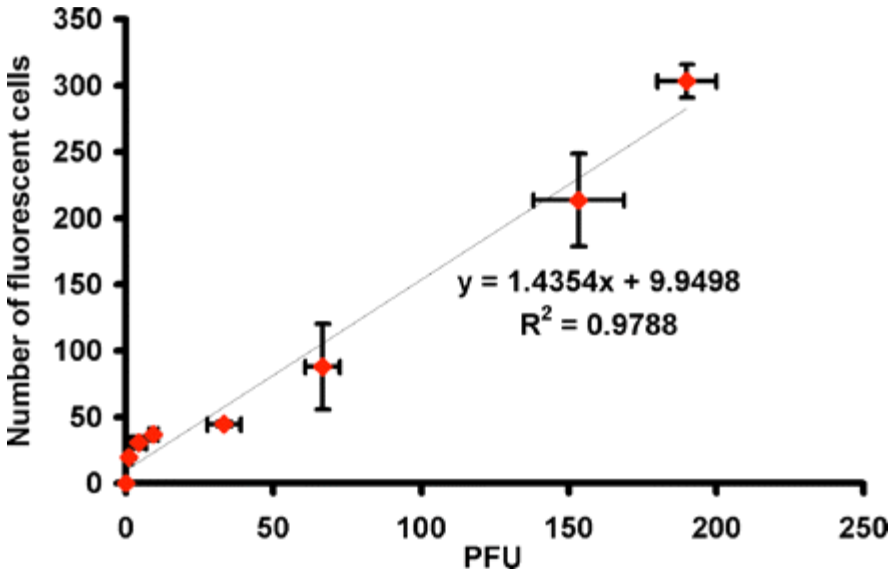
Number of fluorescent cells
350
300
250
200
150
100
50
0
0
50
100
150
200
250
PFU
y = 1.4354x + 9.9498
R2 = 0.9788

Fig. 2.5.

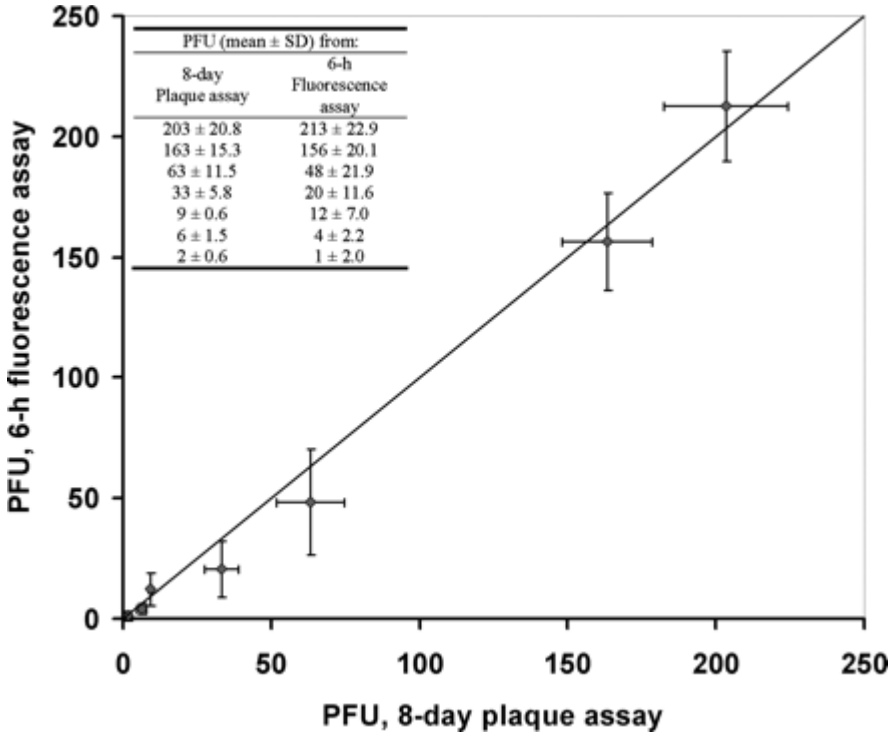
PFU (mean ± SD) from:
8-day Plaque assay
6-h Fluorescence assay
203 ± 20.8
213 ± 22.9
163 ± 15.3
156 ± 20.1
63 ± 11.5
48 ± 21.9
33 ± 5.8
20 ± 11.6
9 ± 0.6
12 ± 7.0
6 ± 1.5
4 ± 2.2
2 ± 0.6
1 ± 2.0
PFU, 6-h fluorescence assay
PFU, 8-day plaque assay
0
50
100
150
200
250

Chapter 3:

Visualizing the dynamics of viral replication in living cells via Tat-peptide delivery of nuclease-resistant molecular beacons

Abstract

This study describes the use of nuclease-resistant molecular beacons (MBs) for the real-time detection of coxsackievirus B6 replication in living Buffalo green monkey kidney (BGMK) cells via Tat peptide delivery. A nuclease-resistant MB containing 2′-O-methyl RNA bases with phosphorothioate internucleotide linkages was designed to specifically target an 18-bp 5′ noncoding region of the viral genome. For intracellular delivery, a cell-penetrating Tat peptide was conjugated to the MB by using a thiol–maleimide linkage. Presence of the Tat peptide enabled nearly 100% intracellular delivery within 15 min. When the conjugate was introduced into BGMK cell monolayers infected with coxsackievirus B6, a discernible fluorescence was observed at 30 min after infection, and as few as 1 infectious viral particle could be detected within 2 h. The stability and the intracellular delivery properties of the modified MBs enabled real-time monitoring of the cell-to-cell spreading of viral infection. These results suggest that the Tat-modified, nuclease-resistant MBs may be powerful tools for improving our understanding of the dynamic behavior of viral replication and for therapeutic studies of antiviral treatments.

Introduction

Real-time detection of mRNA in living cells is essential to provide information on the dynamics of RNA expression and localization and can be an important tool for advancement in disease pathophysiology, drug discovery, and medical diagnostics. In particular, the ability to monitor the real-time replication of viruses in living cells is vital for the rapid detection of viral infection and an understanding of viral pathogenesis.

Among the technologies currently under development for gene detection in living cells, perhaps the most promising one is molecular beacons (MBs). MBs are single-stranded oligonucleotide probes possessing a stem-loop structure; they are double labeled with a fluorophore at one end and a quencher at the other (1). These probes are specific for a target nucleotide sequence and produce fluorescence upon target binding. The spontaneous hybridization between MBs and their target sequences is highly specific and can even distinguish a single nucleotide mismatch (2–4). Recently, MBs have been used to detect the presence of viral RNA in infected cells, with positive responses to even a single infectious viral particle (5). However, the long-term, real-time monitoring of viral RNA in living cells has not been possible because of the relatively short half-life (~30 min) of MBs due to endogenous nuclease degradation, resulting in false-positive signals (6, 7). It has been shown that modifications of MBs with 2′-O-methyl RNA bases and phosphorothioate internucleotide linkages can be used to significantly improve duplex stability and nuclease resistance (8–13). It is easy to envision that such an MB design can be adapted for the real-time monitoring of viral infection.

In addition, real-time monitoring of viral replication using MBs has been hindered by the lack of an efficient and noninvasive method for intracellular delivery. Conventional approaches such as transfection are slow and inefficient. Delivery based on streptolysin O is faster (~2 h) but can be used only in *ex vivo* cellular assays. Even microinjection is not suitable for viral detection, because one cannot predict *a priori* which cells are infected by viruses. Among the many noninvasive intracellular delivery methods, the HIV-1-derived Tat peptide-based method is the most efficient and has been shown to retain the ability to intracellularly deliver various conjugated cargoes (14–16). This Tat-based method, when combined with nuclease-resistant MBs, could provide a powerful means for rapid detection and real-time monitoring of viral replication in living cells with high specificity and sensitivity.

By delivering nuclease-resistant MBs into host cells before viral infection and subsequently tracking fluorescent hybrids with viral RNA, it is envisioned that a better understanding of the dynamic behavior of viral replication could be gained through *in vivo* experiments and could extend to therapeutic studies of antiviral treatments. This study reports the utilization of a nuclease-resistant MB conjugated with a Tat peptide to examine the coxsackievirus B6 (CVB6) viral reproductive cycle in living host cells.

Materials and Methods

BGMK cell culture.

BGMK cells obtained from American Type Culture Collection (passages 50–60) were grown in 400 mL of 1X autoclavable minimum essential medium (AMEM; Irvine Scientific) containing 4 mL of 7.5% $NaHCO_3$, 8 mL of 1 M Hepes, 4 mL of nonessential amino acids (NEAA; Gibco–BRL), 10 mL of A/B-L (1,000 units/mL penicillin, 1,000 units/mL streptomycin, 2 mg/mL kanamycin, 2,000 units/mL nystatin, 80 mM l-glutamine), and 40 mL of FBS (Sigma–Aldrich) at 37°C in a 5% CO_2 atmosphere. PBS [1X PBS = 0.01 M phosphate (pH 7.4), 0.138 M NaCl, and 2.7 mM KCl] and Tris-buffered saline solution [1X TBSS = 0.05 M Tris (pH 7.4), 0.28 M NaCl, 10 mM KCl, and 0.82 mM Na_2HPO_4] were used for washing steps in the plaque assay and MB analysis, respectively.

Virus preparation.

Virus stocks of CVB6 Schmitt strain (ATCC VR-155) were allowed to proliferate on BGMK cells for 2 days at 37°C in a 5% CO_2 atmosphere and collected by freeze–thawing (3 times) infected flasks demonstrating >80% lysis and extracting the cell lysate with chloroform. The CVB6 virus stock was stored at −80°C.

Plaque assay.

The CVB6 virus stock was thawed, and then a series of 10-fold serial dilutions in 1X PBS were prepared. Confluent, 1-day-old BGMK cell monolayers in 12-well, 22.1-mm dishes (Costar; Corning) were infected with 1 mL of virus dilution. After 90 min of adsorption at room temperature, the solutions were aspirated, and 1 mL of 100 mL of 2% carboxymethylcellulose (CMC) sodium salt (Sigma–Aldrich) containing 100 mL of 2X AMEM (Irvine Scientific) with 2 mL of 7.5% $NaHCO_3$, 4 mL of 1M Hepes, 2 mL of NEAA, 5 mL of A/B-L, and 4 mL of FBS (Sigma–Aldrich) was added into each well. After 2 days of incubation at room temperature, the CMC overlay was removed, and the cells were treated with 0.8% crystal violet/3.7% formaldehyde solution overnight. Excess stain was removed by washing with de-ionized water and the virus plaques were counted.

Design of nuclease-resistant MB.

MB CVB6 was designed on the basis of an alignment of the sequences of enterovirus strains obtained from GenBank database. The DNA folding program mfold (www.bioinfo.rpi.edu/) and IDT SciTools (www.idtdna.com/SciTools/SciTools.aspx) were used to predict the thermodynamic properties and the secondary structures of MBs. MB CVB6 5′-6-FAM (fluorescein)-GCCGCTCGCATTCAGGGGCCGGAGAGC/thiol-dG/GC-DABCYL-3′ [stem sequence is underlined; DABCYL is 4-(4-dimethylaminophenylazo)benzoic acid] possessing a 2′-O-methylribonucleotide backbone with phosphorothioate internucleotide linkages was synthesized (TIB Molbiol) to be specifically hybridized to an 18-bp region of the 5′ untranslated region of the

enterovirus genome. The thiol group on the quencher end is for the reaction with a maleimide group attached to the N terminus of the Tat peptide to form a thiol–maleimide bridge. MB CVB6 was suspended in 100 mM Tris·HCl (pH 8.0) buffer containing 1 mM $MgCl_2$ to make the concentration 100 μM for the subsequent studies.

DNase sensitivity.

To test the nuclease sensitivity of MB CVB6, the fluorescence of a 500-μL solution of 1 μM MB CVB6 was recorded as a function of time at room temperature. Five units of ribonuclease-free DNase I was added, and the fluorescent signals (excitation 495 nm, emission 521 nm) were measured for 30 min by using an RF-551 spectrofluorometric detector (Shimadzu). As a comparison, the fluorescence of a 500-μL solution of 1 μM MB possessing deoxyribonucleotide backbones 5′-6-FAM - GCCGCTCGCATTCAGGGGCCGGAGAGCGGC-DABCYL-3′ (MB CVB1, stem sequence is underlined) was recorded after adding 5 units of ribonuclease-free DNaseI. Without adding ribonuclease-free DNase I, the background fluorescent signals of a 500-μL solution containing 1 μM MB CVB6 or MB CVB1 were monitored for 30 min.

Peptide conjugation.

One hundred and fifty micromolar N-terminal maleimide-modified Tat peptide H-Tyr-Gly-Arg-Lys-Lys-Arg-Arg-Gln-Arg-Arg-Arg-N-CH_2CH_2-N-maleimide (Global Peptide) was mixed with 100 μM thiolated MB in the dark for 2 h to form a stable thiol–maleimide linkage. The peptide-linked MB complex was dialyzed overnight in Slide-A-

Lyzer Mini Dialysis Units, 10,000 molecular weight cutoff, to remove the unconjugated peptide/MBs (Pierce). The peptide-conjugated MB CVB6-Tat was stored at −20°C until used for experiments.

Cellular delivery of peptide-conjugated MBs.

BGMK cells were seeded into the 8-well Lab-Tek Chambered Coverglass (Fisher Scientific) at 37°C in 5% CO_2 in air and cultured to >90% confluence. After removal of the incubation medium, the cell monolayer was washed twice with 1X TBSS. To facilitate determining the efficiency of Tat peptide-mediated intracellular delivery, nonconjugated MB CVB6 or MB CVB6-Tat was mixed with complementary oligonucleotides (5′-CTCCGGCCCCTGAATGCG-3′) to the loop region at an MB/oligonucleotide molar ratio of 1:1. BGMK cells were incubated at 37°C in the dark with 1X Leibovitz L-15 medium (Invitrogen) containing either preformed nonconjugated MB CVB6 hybrids or MB CVB6-Tat hybrids at MB concentrations of 0.5, 1, or 2 μM. The Leibovitz L-15 contains no phenol red to eliminate autofluorescence and to increase optical transmission. To record the image, the chamber well was placed on the Zeiss Axiovert 40 CFL inverted fluorescence microscope stage and was marked to permit the repeated observation of the chosen region in the cell monolayer. As soon as the positive fluorescent signals were observed inside the cells, the chamber well was kept on the microscope stage instead of returning it to the 37°C incubator. All assays were carried out over a period of 12 h, and the fluorescence images were taken at intervals of 5 min.

Progression of viral infection in living cells.

BGMK cells were cultured to >90% confluence in the 8-well Lab-Tek Chambered Coverglass (Fisher Scientific) at 37°C in 5% CO_2 atmosphere. After incubation for predetermined time periods, the slides were removed from the 37°C incubator, and the growth medium was aspirated. Following 2 washes with 1X TBSS, the cells were incubated with 1 μM MB CVB6-Tat in 1X Leibovitz L-15 medium (Invitrogen) at 37°C in the dark for 30 min. Without washing away the incubation medium, the chamber wells were oriented on the microscope stage; the cells were infected with 10-fold virus dilutions in 1X Leibovitz L-15 medium and were observed under the Zeiss Axiovert 40 CFL inverted fluorescence microscope at room temperature for 12 h. The fluorescence images were recorded at intervals of 5 min.

Fluorescence microscopy and image processing.

Living cell imaging was performed on a Zeiss Axiovert 40 CFL inverted microscope equipped with a 12-V, 35-W halogen lamp (for the phase-contrast images) and an HBO 50 W/AC mercury lamp (for the fluorescence images). The objectives used were a 5X/0.12 A-Plan, a 10X/0.25 A-Plan, a 20X/0.50 EC Plan-NEOFLUAR, and a 40X/0.50 LD A-Plan (Zeiss). 6-FAM-labeled fluorescent hybrids were detected by using a filter set consisting of a D480/30-nm exciter, a D535/40-nm emitter, and a 505-dichroic long pass beam splitter (Chroma Technology). Images were acquired by using a ProgRes MFscan Monochrome CCD camera (Jenoptik). Both phase-contrast and fluorescence images were analyzed by using Image-Pro PLUS analysis software (Media Cybernetics). All settings

for image processing were kept constant, and the exposure time for image capture was adjusted, if necessary, to maintain output levels similar to those observed under the fluorescence microscope.

Enumeration of fluorescent cells.

To calculate the infected cells (fluorescent cells) in each chamber well, 30 fields within the well were randomly chosen, and the fluorescence images were collected at 100X magnification. The number of fluorescent cells within the area was counted by Image-Pro PLUS analysis software.

Results and Discussion

Design and characterization of nuclease-resistant MB.

An MB (MB CVB6-Tat) targeting an 18-bp region of the 5′ untranslated region of CVB6 was designed. The DNA backbone was modified with sulfur-substituted 2′-O-methyl oligoribonucleotides for improved nuclease resistance (17–20). A Tat peptide for intracellular delivery was conjugated to the thiol group at the quencher end by using a maleimide group placed at the N terminus of the peptide (Fig. 3.1A) (21, 22). As expected, the modified MBs were highly resistant to nuclease cleavage by DNase I (Fig. 3.1B). In contrast, an unmodified MB was susceptible to nuclease degradation, resulting in almost instantaneous increase in fluorescence. The dual modifications had no effect on the hybridization kinetics of the MB, as a rapid increase in fluorescence was observed in the presence of a complementary target (Fig. 3.1C).

Intracellular delivery of Tat-modified MB CVB6.

The intracellular delivery efficiency was tested by incubating 0.5, 1, or 2 μM MB–target hybrids with a monolayer of Buffalo green monkey kidney (BGMK) cells. Fluorescence was detectable in 100% of the living cells as early as 15 min after introduction of the MB–target hybrids (Fig. 3.2A). The time-lapse images showed that the cellular uptake increased after 15 min and reached saturation after 1 h of incubation. The fluorescence intensity was constant for up to 12 h, indicating that the MB–target hybrids were retained inside the cells after delivery and remained resistant to the intracellular RNase H. Unhybridized MB was also introduced into BGMK cells, and no fluorescence was

detected during the same 12-h period, again indicating the intracellular resistance of the modified MBs to nuclease attack (Fig. 3.2B). In contrast, in the absence of Tat, no internalization of MBs was observed, and fluorescence was detected only in the medium (Fig. 3.2B), confirming the effectiveness of the Tat peptide for rapid intracellular delivery.

Detection of CVB6 infection by Tat-modified MBs.

After validating the properties of Tat-modified MBs, their ability to detect viral RNA was tested. A confluent monolayer of BGMK cells was first incubated with 1 μM MB for 30 min before being infected with 10-fold serial dilutions of CVB6, followed by fluorescence microscopy. Compared with uninfected cultures (0 PFU), where no fluorescent cells were present independent of time, a greater number of fluorescent cells were detected at 2 h post infection (p.i.) for the culture infected with a viral dosage corresponding to 1 PFU (Fig. 3.3A). The higher number of fluorescent cells compared with plaque-forming units is likely due to the fact that not all viruses that infect a cell are necessarily able to complete the replication cycle (23). This result is also consistent with the higher infectious virus titers observed by using the quantal assay, which is based on the direct microscopic viewing of cells for virus-induced cytopathic effects, rather than the plaque assay (24). This 2-h detection window is substantially faster than a similar approach reported using cell fixation/permeabilization (16). It is possible that the rapid and noninvasive intracellular delivery enables hybridization with viral RNA to occur shortly after virus uncoating without the possibility of degradation caused by

fixation/permeabilization. To our knowledge, detection of 1 PFU of CVB6, or any other enterovirus, at 2 h p.i. has never been reported.

Using the 2-h infection window, the utility of Tat-modified MBs was tested to quantify infectious CVB6 dosages. Cells were infected with 1–200 PFU of CVB6 per well, and the average number of fluorescent cells was recorded. A linear correlation was obtained by plotting the number of fluorescent cells versus plaque-forming units (Fig. 3.3B). The number of plaque-forming units can be determined easily by using the correlation obtained after direct counting of fluorescent cells. More importantly, the method can be used to provide rapid quantification of infectious CVB6 dosages within 2 h p.i. compared with the minimum 48-h incubation period for the plaque assay.

Real-time monitoring of cell-to-cell spreading of CVB6.

The ability to detect infected cells continuously should allow one to follow the spreading of infectious viruses on a real-time basis. To determine whether this was indeed possible, BGMK cells were infected at a very low infection dosage (multiplicity of infection: 0.01 PFU/cell) and monitored continuously by using a fluorescence microscope in a fixed area for 12 h. Fig. 3.4 shows the cell-to-cell progression of virus spreading at 6 representative time points. Several infected cells were observed at 15 min p.i., suggesting that the viruses entered the cells and started the uncoating process within 15 min. The number of fluorescent cells slowly increased with time, suggesting continuous virus infection. By 6 h p.i., a further outward spread of fluorescent cells was observed, indicating the secondary spreading of infection from progeny virions to cells surrounding the initial

infected cells. The number of fluorescent cells continued to increase with time, and infection spread outward to the entire observation area by 12 h p.i. The majority of infected cells remained adherent and some fluorescence was visible outside the cells, indicating that the fluorescent hybrids with viral RNA entered the extracellular region as a result of the release of progeny virions during cell lysis.

In summary, this study demonstrated the use of nuclease-resistant, Tat-modified MB for real-time monitoring of viral replication and infection. This method is simple because it requires no cell pretreatment (e.g., fixation/permeabilization) and can be used to study cell-to-cell viral spreading. This method is particularly attractive when applied to viruses with very slow growth, nonlytic viruses, and those that do not produce detectable cytopathic effects in infected cells. Compared with conventional viral plaque assays, which detect infection based on cell lysis only and may take days to weeks to complete, this real-time approach provides an opportunity to study the progress of the entire infectious cycle.

References

1. Tyagi, S., and F. R. Kramer. 1996. Molecular beacons: Probes that fluoresce upon hybridization. Nat. Biotechnol. 14:303–308.

2. Marras, S. A., F. R. Kramer, and S. Tyagi. 1999. Multiplex detection of single-nucleotide variations using molecular beacons. Genet. Anal. 14:151–156.

3. Tyagi, S., D. P. Bratu, and F. R. Kramer. 1997. Multicolor molecular beacons for allele discrimination. Nat. Biotechnol. 16:49–53.

4. Tyagi, S., and O. Alsmadi. 2004. Imaging native-actin mRNA in motile fibroblasts. Biophys. J. 87:4153–4162.

5. Yeh, H, Y., Y. C. Hwang, M. V. Yates, A. Mulchandani, and W. Chen. 2008. Detection of hepatitis A virus using a combined cell culture-molecular beacon assay. Appl. Environ. Microbiol. 74:2239–2243.

6. Dirks, R. W., C. Molenaar, and H. J. Tanke. 2001. Methods for visualizing RNA processing and transport pathways in living cells. Histochem. Cell Biol. 115:3–11.

7. Li, J. J., R. Geyer, and W. Tan. 2000. Using molecular beacons as a sensitive fluorescence assay for enzymatic cleavage of single-stranded DNA. Nucleic Acids Res. 28:e52.

8. Bratu, D. P., B. J. Cha, M. M. Mhlanga, F. R. Kramer, and S. Tyagi. 2003. Visualizing the distribution and transport of mRNAs in living cells. Proc. Natl. Acad. Sci. USA 100:13308–13313.

9. Cotton, M., et al. 1991. 2'-O-methyl, 2'-O-ethyl oligoribonucleotides and phosphorothioate oligodeoxyribonucleotides as inhibitors of the in vitro U7 snRNP-dependent mRNA processing event. Nucleic Acids Res. 19:2629–2635.

10. Fisher, T. L., T. Terhorst, X. Cao, and R. W. Wagner. 1993. Intracellular disposition and metabolism of fluorescently-labeled unmodified and modified oligonucleotides microinjected into mammalian cells. Nucleic Acids Res. 21:3857–3865.

11. Iyer, R. P., W. Egan, J. B. Regan, and S. L. Beaucage. 1990. 3H-1,2-Benzodithiole-3-one 1,1-dioxide as an improved sulfurizing reagent in the solid-phase synthesis of oligodeoxyribonucleoside phosphorothioates. J. Am. Chem. Soc. 112:1253–1254.

12. Molenaar, C., et al. 2001. Linear 2'-O-methyl RNA probes for the visualization of RNA in living cell. Nucleic Acids Res. 29:e89.

13. Tsuji, A., et al. 2000. Direct observation of specific messenger RNA in a single living cell under a fluorescence microscope. Biophys. J. 78:3260–3274.

14. Deshayes, S., M. C. Morris, G. Divita, and F. Heitz. 2005. Cell-penetrating peptides: Tools for intracellular delivery of therapeutics. Cell Mol. Life Sci. 62:1839–1849.

15. Saalik, P., et al. 2004. Protein cargo delivery properties of cell-penetrating peptides. A comparative study. Bioconjugate Chem. 15:1246–1253.

16. Wang, A., A. M. Salazar, M. V. Yates, A. Mulchandani, and W. Chen. 2005. Visualization and detection of infectious coxsackievirus replication using a combined cell culturemolecular beacon assay. Appl. Environ. Microbiol. 71:8397–8401.

17. Cook, P. D. 1991. Medicinal chemistry of antisense oligonucleotides–future opportunities. Anticancer Drug Des. 6:585–607.

18. Eckstein, F. 1985. Nucleoside phosphorothioates. Annu. Rev. Biochem. 54:367–402.

19. Iribarren, A. M., et al. 1990. 2’-O-alkyl oligoribonucleotides as antisense probes. Proc. Natl. Acad. Sci. USA 87:7747–7751.

20. Tsourkas, A., M. A. Behlke, and G. Bao. 2002. Hybridization of 2'-O-methyl and 2'-deoxy molecular beacons to RNA and DNA targets. Nucleic Acids Res. 30:5168–5174.

21. Haugland, R. P. 2005. The Handbook. A Guide to Fluorescent Probes and Labeling Technologies (Invitrogen, Eugene, OR), 10th Ed, pp 95–97.

22. Nitin, N., P. J. Santangelo, G. Kim, S. Nie, and G. Bao. 2004. Peptide-linked molecular beacons for efficient delivery and rapid mRNA detection in living cells. Nucleic Acids Res. 32:e58.

23. Dulbecco, R., and H. S. Ginsberg. 1980. Virology (Harper & Row, Philadelphia).

24. Dahling, D. R. 2002. An improved filter elution and cell culture assay procedure for evaluating public groundwater systems for culturable enteroviruses. Water Environ. Res. 74:564–568.

Legends to Figures

Fig. 3.1. MB backbone modification and nuclease sensitivity study. (A) A schematic representation of the Tat-modified, nuclease-resistant MB. The phosphodiester bond was modified by replacing a nonbridging oxygen with sulfur and the 2′-sugar deoxy with 2′-O-methyl group. At room temperature, the thiol group at the quencher end reacted (~2 h) with a maleimide group placed at the N terminus of the peptide to yield a chemically stable thioether bond. (B) Nuclease sensitivity assays using ribonuclease-free DNase I. The fluorescence of the nuclease-resistant MB is shown in red, and the fluorescence of an unmodified MB is shown in green. The background fluorescent signals (shown in black and yellow) without DNase I addition are also shown. (C) Kinetics of hybridization of Tat-modified MB CVB6 with (black) or without (red) complementary oligonucleotides.

Fig. 3.2. Intracellular delivery of MB CBV6-Tat–target hybrids (A) or MB without Tat modification or without targets. (B) BGMK cells were incubated with 1 μM MB for 12 h, and images were captured by using a fluorescent microscope. Scale bar, 20 μm.

Fig. 3.3. *In vivo* detection of CVB6 in BGMK cells. (A) Visualization of BGMK cells infected with 0, 1, or 10^5 PFU at 2 h p.i. (B) The correlation between the number of plaque-forming units and fluorescent cells at 2 h p.i. Error bars represent the standard deviation of 3 replicate experiments. Scale bar, 40 μm.

Fig. 3.4. Real-time detection of viral spreading. BGMK cells were first incubated with 1 μM MB, infected with CVB6 at a multiplicity of infection of 0.01 PFU/cell, and monitored by using a fluorescent microscope. Scale bar, 20 μm.

Fig. 3.1A.

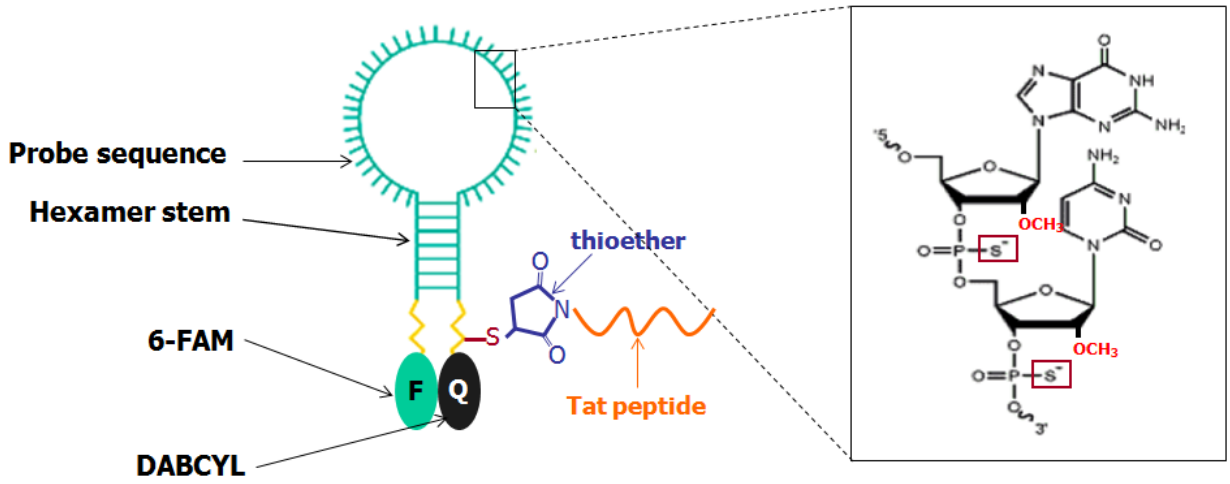

Fig. 3.1B.

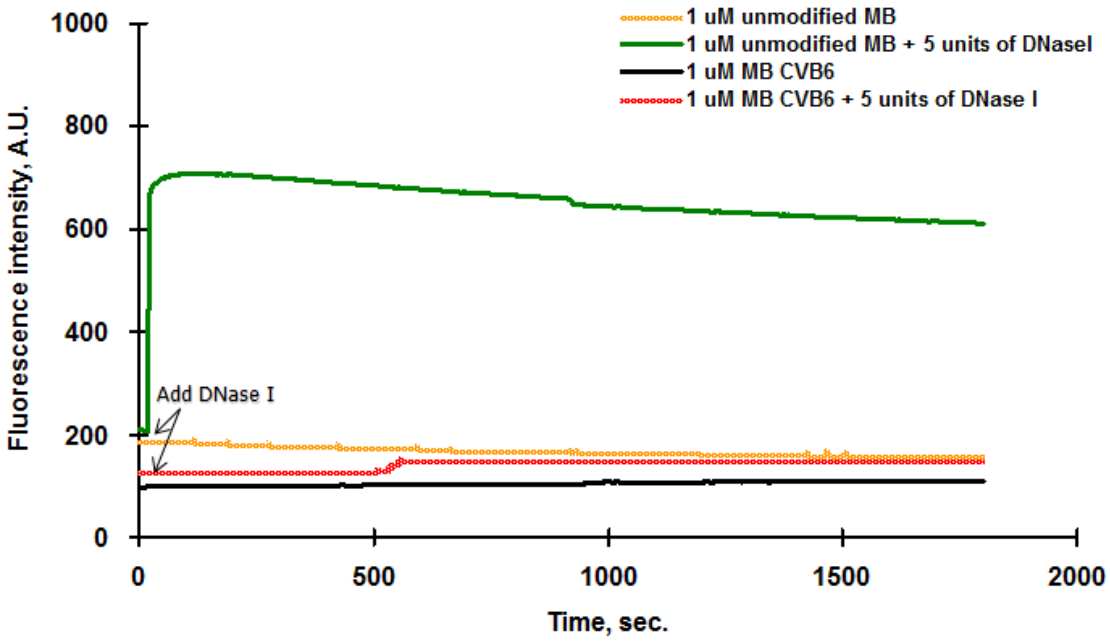

Fig. 3.1C.

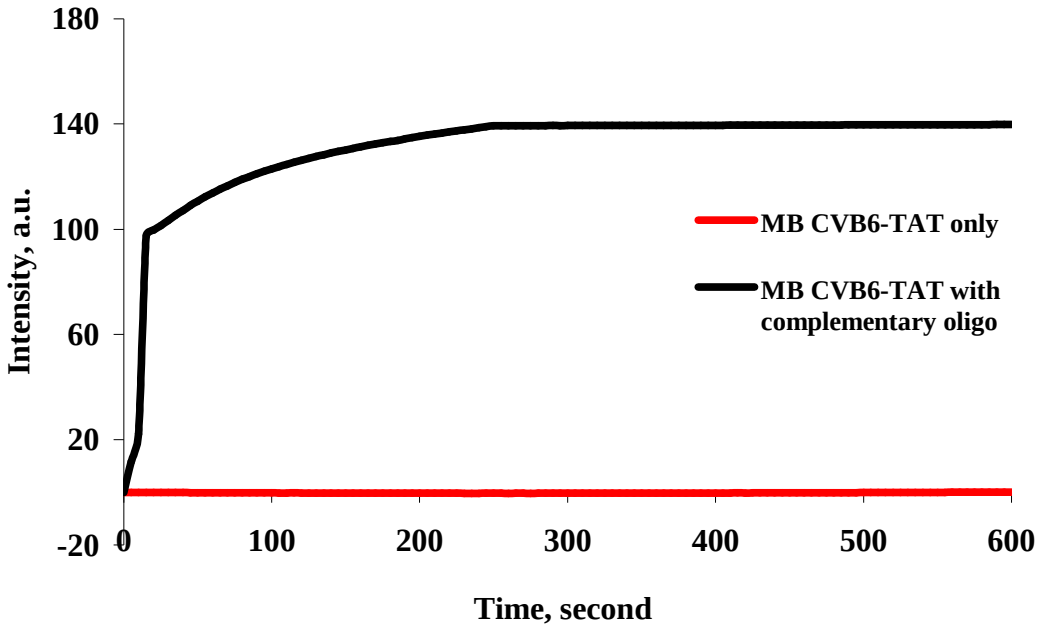
180
140
100
60
20
-20
Intensity, a.u.
0
100
200
300
400
500
600
Time, second
MB CVB6-TAT only
MB CVB6-TAT with complementary oligo

Fig. 3.2A.

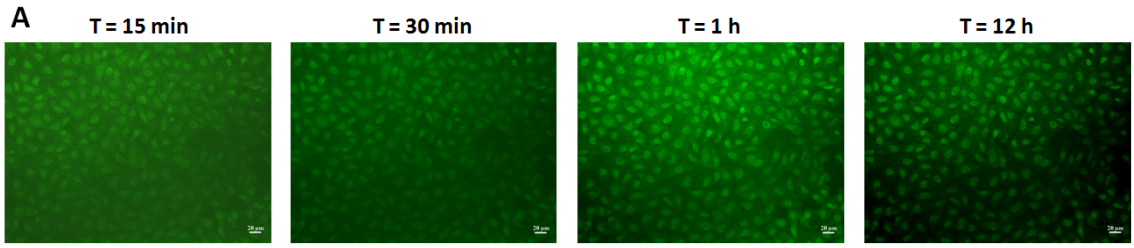

Fig. 3.2B.

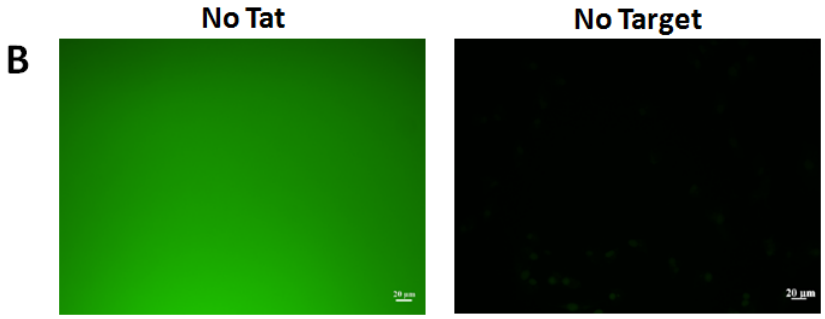

Fig. 3.3A.

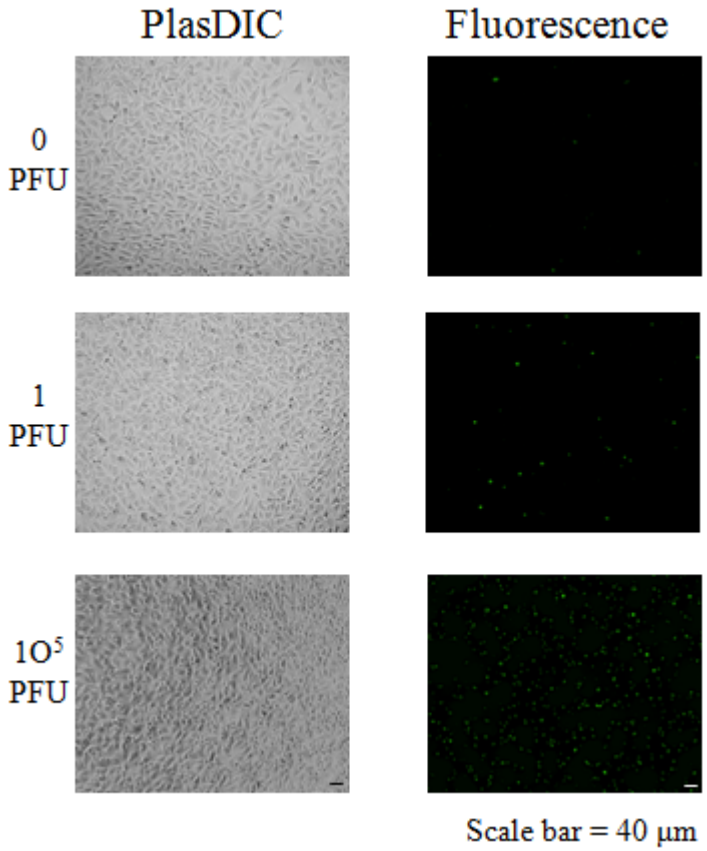

Fig. 3.3B.

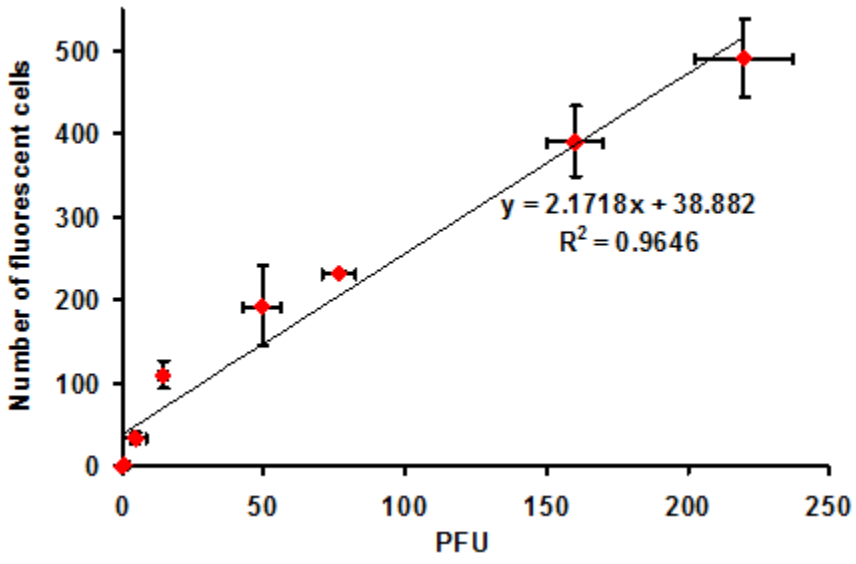

Fig. 3.4.

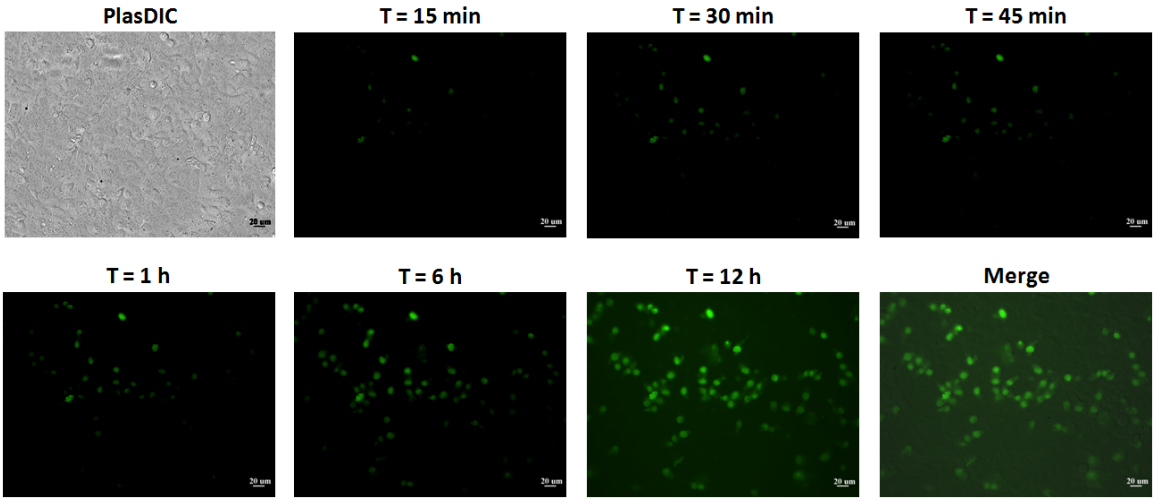

Chapter 4:

Molecular beacon-quantum dot-Au nanoparticle hybrid nanoprobes for visualizing virus replication in living cells

Abstract

This study describes a new hybrid fluorescent nanoprobe composed of a nuclease-resistant molecular beacon (MB) backbone, CdSe-ZnS core-shell quantum dots (QDs) as donors, and gold nanoparticles (Au NPs) as quenchers, for the real-time visualization of virus replication in living cells. A thiol-reactive hexahistidine linker was first conjugated to thioated-MBs. The presence of mono-sulfo-NHS esters on the surface of Au NPs enabled their facile attachment to the peptide-MB conjugates via the 3' amino group on the MB. Finally, the Au NP-MB conjugates were self-assembled onto the QD via the strong metal-affinity coordination between the polyhistidine and the ZnS shell. By using a Au NP-MB to QD ratio of 6:1, a 7.3-fold increase in fluorescent signal was achieved upon target binding. For living cell experiments, a hexahistidine-appended Tat peptide was self-assembled onto the QD surface to provide nearly 100% non-invasive delivery of the QD-MB-Au NP probes within 2 h. By directly visualizing the fluorescent complexes formed with the newly synthesized viral RNA, this QD-MB-Au NP probe provided sensitive and real-time detection of infectious viruses. The number of fluorescent cells increased in a viral dose-responsive manner that enabled the quantification of infectious virus particles as well as the real-time visualization of cell-to-cell virus spreading. This new nanoprobe can be easily adaptable for the real-time visualization of gene expression that are critical for understanding the infection process, enabling a wide range of biotechnology applications and medical diagnostics.

Introduction

The ability to provide real-time intracellular monitoring of gene expression for an extended period of time is becoming increasingly important for neurological studies, cell differentiation, cancer diagnostics, drug discovery, and pathophysiology (1-5). In particular, real-time detection of viral genomes in living cells is essential to gain insights into the molecular mechanisms involved in the viral reproductive cycle (e.g., entry, replication, and egress), the cell-to-cell spread of progeny virions, and for rapid clinical diagnostics. Among the various methods reported to date, molecular beacons (MBs) are considered one of the most promising technologies currently under development for real-time gene detection. MBs are single-stranded oligonucleotides with a hairpin structure that fluoresce upon hybridizing to the target sequence via fluorescence resonance energy transfer (FRET) (6-9). Although MBs have been used for intracellular detection of gene expression, their applications for viral detection in infected cells have only been reported recently (10). The major challenges in using the conventional MB for *in vivo* viral detection are their modest half-life (~50 min) due to cytoplasmic nuclease degradation and a lack of non-invasive intracellular delivery (11-12). Recently, the use of nuclease-resistant MBs for the real-time detection of coxsackievirus replication in living cells via Tat peptide delivery was reported elsewhere (13). The enhanced stability and the non-invasive delivery also enabled real-time monitoring of cell-to-cell spreading of viral infection.

Despite the very exciting possibility of improving our understanding on viral infection, one major limitation of conventional MBs is their use of organic fluorophores,

which have low resistance to photodegradation, rendering them ineffective for long-term monitoring (14). Semiconductor quantum dots (QDs) are inorganic fluorophores that can circumvent the limitations encountered with organic fluorophores. They are brighter and more resistant to photodegradation (up to 100 times) than organic fluorophores (15) and these properties make them excellent probes for single-molecule observation over an extended period of time (16). Their broad absorption spectra and narrow emission peaks also allow the simultaneous excitation of different QDs at a single wavelength for multiplex detection (17). All of these advantages make QDs an attractive alternative for *in vivo* imaging in living cells and live animals (18-21).

QD-based MBs using organic quenchers such as the black hole quencher BHQ2 or Cy5 have recently been reported (22-23). In both cases, less than a 100% increase in the QD fluorescence was observed upon hybridization with a target sequence. This relatively modest increase is a result of inefficient quenching afforded by BHQ2 and Cy5. It has been shown that the emission of QDs can be more effectively quenched using Au nanoparticles (NPs) than most conventional organic quenchers (24-25). Within the typical FRET separation distance, the quenching efficiency can be over an order of magnitude better for Au NPs (26), and Qd-Au NP nano assemblies with a quenching efficiency close to 100% have been reported (27). One can envision that the use of QD and Au NP as the FRET pair for MBs will significantly improve not only the prospect for long-term monitoring of gene expression in living cells or animals, but also the sensitivity due to the improved signal-to-noise ratio.

Materials and Methods

BGMK cell culture.

BGMK cells obtained from American Type Culture Collection (passages 50–60) were grown in 400 mL of 1X autoclavable minimum essential medium (AMEM; Irvine Scientific) containing 1% of 7.5% $NaHCO_3$, 2% of 1 M Hepes, 1% of nonessential amino acids (NEAA; HyClone, Thermo Scientific), 100 µg/mL of penicillin and 100 U/mL of streptomycin (HyClone, Thermo Scientific), 1% of 200 mM L-glutamine in 0.85% NaCl (HyClone, Thermo Scientific), and 10% of FBS (Sigma–Aldrich) at 37°C in a 5% CO_2 atmosphere. PBS [1X PBS = 0.01 M phosphate (pH 7.4), 0.138 M NaCl, and 2.7 mM KCl] and Tris-buffered saline solution [1X TBSS = 0.05 M Tris (pH 7.4), 0.28 M NaCl, 10 mM KCl, and 0.82 mM Na_2HPO_4] were used for washing steps in the plaque assay and MB analysis, respectively.

Virus preparation.

Virus stocks of Coxsackie B6 (CVB6) Schmitt strain (ATCC VR-155) were allowed to proliferate on BGMK cells for 2 days at 37°C in a 5% CO_2 atmosphere and collected by freeze–thawing (3 times) infected flasks demonstrating >80% lysis and extracting the cell lysate with chloroform. The CVB6 virus stock was stored at −80°C.

Plaque assay.

The CVB6 virus stock was thawed, and then a series of 10-fold serial dilutions in 1X

PBS were prepared. Confluent, 1-day-old BGMK cell monolayers in 12-well, 22.1-mm dishes (Costar; Corning) were infected with 1 mL of virus dilution. After 90 min of adsorption at room temperature, the solutions were aspirated, and 2% carboxymethylcellulose (CMC) sodium salt (Sigma–Aldrich) containing 1 volume of 2X AMEM (Irvine Scientific) with 2% of 7.5% $NaHCO_3$, 4% of 1 M Hepes, 2% of NEAA, 200 µg/mL of penicillin and 200 U/mL of streptomycin, 2% of 200 mM L-glutamine in 0.85% NaCl (HyClone, Thermo Scientific), and 4% of FBS (Sigma–Aldrich) was added into each well. After 3 days of incubation at room temperature, the CMC overlay was removed, and the cells were treated with 0.8% crystal violet/3.7% formaldehyde solution overnight. Excess stain was removed by washing with de-ionized water and the virus plaques were counted.

Design of nuclease-resistant MB CVB6.

MB CVB6 was designed on the basis of an alignment of the sequences of enterovirus strains obtained from GenBank database. The DNA folding program *mfold* (www.bioinfo.rpi.edu/) and *IDT SciTools* (www.idtdna.com/SciTools/SciTools.aspx) were used to predict the thermodynamic properties and the secondary structures of MBs. MB CVB6 5′-SH-CGCACC***GTAGTC***CGCATTCAGGGGCCGGAG***GACTAC***CAATTA -NH-3′ (probe sequence is underlined and stem sequence is bold italic) possessing a 2′-*O*-methylribonucleotide backbone with phosphorothioate internucleotide linkages was synthesized (TIB Molbiol) to be specifically hybridized to an 18-bp region of the 5′ untranslated region of the enterovirus genome. The thiol group at the 5’ end is for the

reaction with a maleimide group attached to the N terminus of the $(His)_6$ peptide (Pi Proteomics, LLC) to form a thiol–maleimide bridge. The 3' amino-labeled end forms covalent amide linkage with the mono-sulfo-NHS ester on the surface of Au nanoparticles (NPs). MB CVB6 was suspended in 100 mM Tris·HCl (pH 8.0) buffer containing 1 mM $MgCl_2$ to make the concentration 100 μM for the subsequent studies.

Peptide.

One hundred and fifty micromolar N-terminal maleimide-modified H-$(His)_6$- NH-CH_2-CH_2-N-maleimide (Pi Proteomics, LLC) suspended in 10 mM Hepes buffer containing 1 mM $MgCl_2$ was mixed with 100 μM thiolated MB CVB6 in the dark for 2 h to form a stable thiol–maleimide linkage. The peptide-linked MB complex was dialyzed overnight in Slide-A-Lyzer Mini Dialysis Units 10,000 molecular weight cutoff (MWCO) to remove the unconjugated peptide/MBs (Pierce).

QD-MB CVB6-Au NP conjugation.

Several steps were taken to attach QD and Au NP to MB CVB6 in 10 mM Hepes containing 1 mM $MgCl_2$ buffer at pH 8.5 in the ambient environment. To make colloidal QDs compatible with biological environments, the TOP/TOPO capped CdSe-ZnS QDs (Evident Technologies, Inc., NY) were cap-exchanged with dihydrolipoic acid (DHLA) ligands to replace the hydrophobic shell. The basic procedure followed for DHLA-capping is described by Clapp et al. After the QD surface replacement, the DHLA-capped QDs were resuspended in 10 mM Hepes buffer. To form a thiol–maleimide bridge, the

thiol group at the 5’ end of MB sequence reacted with a maleimide group attached to the N terminus of the $(His)_6$ peptide (Pi Proteomics, LLC) as described above. The Mono-Sulfo-NHS-NANOGOLD (Nanoprobes, NY) reagent was dissolved and mixed with MB CVB6 at molar ratio of 2:1 in 200-μL 10 mM Hepes buffer. The 3’ amino-labeled end on the MB sequence formed covalent amide linkage with the mono-sulfo-NHS ester on the surface of Au NPs. The mixture was incubated for 1 h to allow the reaction of sulfo-NHS ester with 3’ amino group on MB CVB6 and then quenched with 10 μL of 10 mM glycine to deactivate any remaining NHS on the NP surface. Unreacted MB sequences and NPs were removed by spin dialysis in Millipore Microcon 10,000 MWCO at 7000×g for 5 min and the NP-labeled MB solution was resuspended in 200-μL 10 mM Hepes buffer. DHLA-capped QD solution was mixed with an increasing molar ratio of NP-labeled MB solution for 1 h in 200-μL 10 mM Hepes buffer. The $(His)_6$ peptide linker at the 5’ end of MB CVB6 facilitated the self-assembly of MB onto the QD surface via metal-affinity interactions. After conjugation, the QD emission spectra of a 100-μL QD-MB-Au NP solution (QD concentration 0.1 μM) were measured on an RF-551 spectrofluorometric detector (Shimadzu, MD) from 450 to 650 nm with a fixed excitation wavelength of 400 nm. For AFM imaging and *in vivo* experiments the desirable concentrations are described below. All QD-based MBs were stored in the dark at 4 °C and were used within 1 day. For intracellular delivery, the $(His)_6$-appended Tat peptides were self-assembled onto the QD surface via metallic affinity as described in section “Cellular Delivery of QD-based MBs”.

AFM (Atomic Force Microscopy) imaging.

The QD-MB-Au NP construct was diluted to 2.5 nM in 10 mM Hepes, pH ~8 and 10 μL of sample was dropped on HOPG surface. After 20-min adsorption, HOPG surface was rinsed with 5-mL DI water and the sample was dried under N_2 flux. AFM images were obtained with a Veeco diInnova (Veeco, CA) in tapping mode using FESP silican cantilever (resonance frequency: ~73 kHz; scan rate 0.2 Hz) and analyzed using diSPMLab Vr.5.01 software (Veeco, CA).

Cellular delivery of QD-based MBs.

For intracellular delivery, the hexahistidine-appended Tat peptide H-$(His)_6$-Trp-Gly-Leu-Ala-Aib-**Tyr-Gly-Arg-Lys-Lys-Arg-Arg-Gln-Arg-Arg-Arg**-$CONH_2$ was synthesized (Pi Proteomics, LLC), where Aib is α-aminoisobutyric acid. The peptide solution was mixed with QD-MB-Au NP solution for 1 h at room temperature in 200-μL 10 mM Hepes buffer at molar ratio of 10:1. $(His)_6$-expressed peptides can be directly attached to the QD-surface based on the strong interaction between Zn^{2+} and histidine. BGMK cells were seeded into the 8-well Lab-Tek Chambered Coverglass (Fisher Scientific) at 37°C in 5% CO_2 in air and cultured to >90% confluence. After removing the incubation medium, the cell monolayer was washed twice with 1X TBSS. To facilitate determining the efficiency of Tat peptide-mediated intracellular delivery, nonconjugated QD-based MB CVB6 or QD-based MB CVB6-Tat was mixed with complementary oligonucleotides (5′-CTCCGGCCCCTGAATGCG-3′) to the loop region at an MB/oligonucleotide molar ratio of 1:1. BGMK cells were incubated at 37°C in the dark with 1X Leibovitz L-15

medium (Invitrogen) containing either preformed nonconjugated QD-based MB CVB6 hybrids or QD-based MB CVB6-Tat hybrids at QD concentrations of 50 nM. To record the image, the chamber well was placed on the Zeiss Axiovert 40 CFL inverted fluorescence microscope stage and was marked to permit the repeated observation of the chosen region in the cell monolayer. As soon as the positive fluorescent signals were observed inside the cells, the chamber well was kept on the microscope stage instead of returning it to the 37°C incubator. All assays were carried out over a period of 12 h, and the fluorescence images were taken at intervals of 15 min.

Progression of viral infection in living cells.

BGMK cells were cultured to >90% confluence in the 8-well Lab-Tek Chambered Coverglass (Fisher Scientific) at 37°C in 5% CO_2 atmosphere. After incubation for predetermined time periods, the slides were removed from the 37°C incubator, and the growth medium was aspirated. Following 2 washes with 1X TBSS, the cells were incubated with 50 nM QD-based MB CVB6-Tat in 1X Leibovitz L-15 medium (Invitrogen) at 37°C in the dark for 3 h. After 2 washes with 1X TBSS, the chamber wells were oriented on the microscope stage; the cells were infected with 10-fold virus dilutions in 1X Leibovitz L-15 medium and were observed under the Zeiss Axiovert 40 CFL inverted fluorescence microscope at room temperature for 12 h. The fluorescence images were recorded at intervals of 15 min. For the real-time spreading of viruses experiment, snapshots were taken from 30 min p.i. to 12.5 h p.i.. From 30 min p.i. to 2.5 hours p.i., they were taken every 15 min; thereafter they were taken every 30 min.

Fluorescence microscopy and image processing.

Living cell imaging was performed on a Zeiss Axiovert 40 CFL inverted microscope equipped with a 12-V, 35-W halogen lamp (for the phase-contrast images) and an HBO 50 W/AC mercury lamp (for the fluorescence images). The objectives used were a 5X/0.12 A-Plan, a 10X/0.25 A-Plan, a 20X/0.50 EC Plan-NEOFLUAR, and a 40X/0.50 LD A-Plan (Zeiss). Fluorescent hybrids were detected by using a filter set consisting of a D436-nm exciter, a D535/50-nm emitter, and a 475 nm-dichroic long pass beam splitter (Chroma Technology). Images were acquired by using a ProgRes MF^{scan} Monochrome CCD camera (Jenoptik). Both phase-contrast and fluorescence images were analyzed by using Image-Pro PLUS analysis software (Media Cybernetics). All settings for image processing were kept constant, and the exposure time for image capture was adjusted, if necessary, to maintain output levels similar to those observed under the fluorescence microscope.

Enumeration of fluorescent cells.

To calculate the infected cells (fluorescent cells) in each chamber well, 30 fields within the well were randomly chosen, and the fluorescence images were collected at 100X magnification. The number of fluorescent cells within the area was counted by Image-Pro PLUS analysis software.

Results and Discussion

This study reports the development of nuclease-resistant MBs using QD and Au NP as the FRET pair for real-time *in vivo* viral detection via Tat peptide delivery. Coxsackievirus B6 (CVB6) was chosen as the virus model considering its importance in waterborne diseases and outbreaks. A nuclease-resistant MB targeting an 18-bp non-coding region of the CVB6 genome was designed similar to that reported previously (13) except for the inclusion of a thiol group at the 5' end and an amino group at the 3' end. A 12-bp linker sequence was inserted at the 3'end to act as a spacer between the MB and the Au NP. To synthesize the QD-MB-Au NP probes (Fig. 4.1), a maleimide-modified hexahistidine (His_6) peptide linker was first conjugated with the free 5' thiol group of the MB to form a stable thioether. The presence of mono-sulfo-NHS esters on the surface of Au NPs enabled their facile attachment to the peptide-MB conjugates via the 3' amino group on the MB. Finally, self assembly of the Au NP-MB conjugates onto DHLA-capped QDs was accomplished via the strong metal-affinity coordination between the ZnS shell and the $(His)_6$ tag.

The QD emission at 540 nm was measured to follow the QD-MB-Au NP conjugation (Fig. 4.2A). The emission peak before DHLA-capping was detected at 540 nm and was red shifted to 548 nm after DHLA replacement as reported previously (28). The effect of QD quenching was investigated by incubating a fixed concentration of QD (0.1 µM) with an increasing molar ratio of Au NP-labeled MB from 1 to 6. Nearly a 40% loss in QD emission was achieved even with an Au NP/QD ratio of 1. This result confirms the correct assembly of Au NP-MB conjugates onto QDs based on the $(His)_6$

interaction, resulting in the efficient quenching of the QD via donor-quencher FRET. A sequential increase in QD quenching was observed with an increasing MB to QD molar ratio up to 6:1 where over 85% loss in the QD photoluminescence was detected. Since only a marginal increase in quenching was observed beyond the ratio of 6:1, this particular Au NP-MB-QD preparation was chosen for subsequent characterization and *in vivo* experiments. To ensure that the modifications with QD and Au NP had no effect on the hybridization kinetics, an excess amount of complementary oligos was added. Fig. 4.2B shows the time-course recovery of QD emission in the presence of complementary oligos. The QD fluorescence intensity upon target binding was enhanced up to 7.3 times within 50 min, which is significantly higher than the 2-3 fold increase reported previously for other QD-based MB conjugates (25). This improvement in the signal to background ratio is likely a combination of using Au NP as the quencher and the insertion of a 12-bp linker, which provides greater separation of Au NPs from the QD surface upon hybridization. This improved signal to background ratio should render the newly designed QD-MB-Au NP probe highly useful for cellular imaging of gene expression.

The QD-MB-Au NP probes hybridized with complementary oligos were further characterized by atomic force microscopy (AFM) imaging with a dilute dispersion of the hybridized MBs on a highly orientated pyrolytic graphite (HOPG) surface. The tapping mode AFM image shows that the oblong shaped QDs were surrounded by a number of smaller Au NPs (Fig. 4.3A). The height profile confirmed the presence of two nanoparticles of approximately 7 nm and 1.4 nm, which are comparable with the respective sizes of a single QD and Au NP specified by the manufacturer. The spacing of

14 nm between the two nanoparticles also corresponded to the opened 42 base pair MB, confirming that the QD was separated from the Au NP by hybridization. In contrast, without the complementary oligos, no separation from the cross-sectional height profile was detected (Fig. 4.3B).

After confirming the expected properties of the QD-MB-Au NP probes, Tat peptides were appended to the QD surface via coordination with the His_6-tag at a ratio of 10:1. To investigate the intracellular delivery efficiency, QD-MB-Au NP probes appended with Tat peptides were first hybridized with an excess amount of complementary oligos before being added to a monolayer of Buffalo green monkey kidney (BGMK) cells. As depicted in Fig. 4.4A, intracellular delivery occurred within 1 h and the level of delivery continued to increase with time until reaching saturation at 6 h. The fluorescent intensity was constant for up to 12 h, indicating that the MB-target hybrids were retained inside the cells after delivery and remained resistant to intracellular degradation. In the absence of Tat peptide conjugation, rapid aggregation of the probes occurred outside the cells (Fig. 4.4B). After washing away the medium, there was no significant fluorescence detected inside the cells, confirming that the conjugates were not taken up by the cells without the help of Tat peptides.

To demonstrate the ability of the Tat-modified QD-MB-Au NP probes to monitor the infection state of individual cells, a confluent monolayer of BGMK cells was first incubated with 50 nM probes for 3 h before being infected with 0 to 10^3 plaque forming unit (PFU) of CVB6. The number of fluorescent cells was followed by fluorescence microscopy after 4 h of infection. As shown in Fig. 4.5A, a significantly higher number

of fluorescent cells was detected with increasing infection dosages, while the uninfected cultures (0 PFU) showed a negligible amount of fluorescence (background) independent of infection time (Fig. 4.5A). Using the 4 h infection window, a linear calibration curve was obtained over the range of 1 to 200 PFU (Fig. 4.5B), indicating that this QD-based MB assay can be used to provide rapid quantitative information on infectious viral dosages without performing the tedious 72-h plaque assay.

By delivering the probe complex into cells prior to viral infection and subsequently tracking the increase in fluorescent signals, this method provides the feasibility for the real-time detection of newly synthesized viral RNA and the cell-to-cell spreading of viral infection. A cell monolayer was infected at a multiplicity of infection (M.O.I.) of 0.1 PFU/cell and monitored under a fluorescence microscope for 12 h. After 3 h infection (Fig. 4.6A), several fluorescent cells were clearly observable under the microscope. As time proceeded, the fluorescent intensity inside these infected cells became more intense, indicating that continual RNA synthesis and virus assembly was occurring. The further outward spread of fluorescent cells at 8 h p.i. indicated secondary infection caused by the progeny virions. In contrast, no noticeable increase in fluorescent cells was detected in a control culture without infection even after 12 h (Fig. 4.6B). This control experiment showed that the probes are stable and nuclease-resistant. These results confirm the intracellular stability of the QD-MB-Au probes and their ability to provide real-time detection of viral infection.

In summary, this study demonstrated the utilization of nuclease-resistant QD-MB-Au NP probes to examine the viral replication cycle in living host cells via Tat peptide

delivery. Our findings indicate that this new MB probe design can be used to explore many real-time molecular mechanisms that are critical for understanding virus-host interactions and viral pathogenesis.

References

1. Cros, J. F., and Palese, P. 2003. Trafficking of viral genomic RNA into and out of the nucleus: influenza, Thogoto and Borna disease viruses. Virus Res. 95:3-12.

2. Cui, Z. Q., Z. P. Zhang, X. E. Zhang, J. K. Wen, Y. F. Zhou, and W. H. Xie. 2005. Visualizing the dynamic behavior of poliovirus plus-strand RNA in living host cells. Nucleic Acids Res. 33:3245–3252.

3. Duprex, W. P., S. McQuaid, L. Hangartner, M. A. Billeter, and B. K. Rima. 1999. Observation of measles virus cell-to-cell spread in astrocytoma cells by using a green fluorescent protein-expressing recombinant virus. J. Virol.73:9568–9575.

4. McDonald, D, M. A. Vodicka, G. Lucero, T. M. Svitkina, G. G. Borisy, M. Emerman, and T. J. Hope. 2002. Visualization of the intracellular behavior of HIV in living cells. J. Cell Biol. 159:441–452.

5. Pickard, G. E., C. A. Smeraski, C. C. Tomlinson, B. W. Banfield, J. Kaufman, C. L. Wilcox, L. W. Enquist, and P. J. Sollars. 2002. Intravitreal injection of the attenuated pseudorabies virus PRV Bartha results in infection of the hamster suprachiasmatic nucleus only by retrograde transsynaptic transport via autonomic circuits. J. Neurosci. 22:2701–2710.

6. Marras, S. A. E., F. R. Kramer, and S. Tyagi. 1999. Multiplex detection of single-nucleotide variations using molecular beacons. Genet. Anal-Bionol. E. 14:151-156.

7. Tyagi S., and F. R. Kramer. 1996. Molecular beacons: probes that fluoresce upon hybridization. Nat. Biotech. 14:303-308.

8. Tyagi S., D. P. Bratu, and F. R. Kramer. 1998. Multicolor molecular beacons for allele discrimination. Nat. Biotech. 16:49-53.

9. Tyagi S., and O. Alsmadi. 2004. Imaging Native β-Actin mRNA in Motile Fibroblasts. Biophys. J. 87:4153–4162.

10. Yeh, H, Y., Y. C. Hwang, M. V. Yates, A. Mulchandani, and W. Chen. 2008. Detection of hepatitis A virus using a combined cell culture-molecular beacon assay. Appl. Environ. Microbiol. 74:2239–2243.

11. Bratu, D. P., B.-J. Cha, M. M. Mhlanga, F. R. Kramer, and S. Tyagi. 2003. Visualizing the distribution and transport of mRNAs in living cells. Proc. Natl. Acad. Sci. USA 100:13308–13313.

12. Cotten, M., B. Oberhauser, H. Brunar, A. Holzner, G. Issakides, C. R. Noe, G. Schaffner, E. Wagner, and M. L. Birnstiel. 1991. 2'-O-methyl, 2'-O-ethyl

oligoribonucleotides and phosphorothioate oligodeoxyribonucleotides as inhibitors of the in vitro U7 snRNP-dependent mRNA processing event. Nucleic Acids Res. 19:2629–2635.

13. Yeh, H. Y., M. V. Yates, A. Mulchandani, and W. Chen. 2008. Visualizing the dynamics of viral replication in living cells via Tat peptide delivery of nuclease-resistant molecular beacons. Proc. Natl. Acad. Sci. USA. 105:17522-17525.

14. Hermanson, G. T. Bioconjugate Techniques, Academic Press, London, 1996, ch. 8

15. Goldman, E. R., G. P. Anderson, P. T. Tran, H. Mattoussi, P. T. Charles, and J. M. Mauro. 2002. Conjugation of luminescent quantum dots with antibodies using an engineered adaptor protein to provide new reagents for fluoroimmunoassays. Anal. Chem. 74:841–847.

16. Michalet, X., F. F. Pinaud, L. A. Bentolila, J. M. Tsay, S. Doose, J. J. Li, G. Sundaresan, A. M. Wu, S. S. Gambhir, and S. Weiss. 2005. Quantum dots for living cells, *in vivo* imaging, and diagnostics. Science. 307:538-544.

17. Chan, W., and N. Shuming. 1998. Quantum Dot Bioconjugates for Ultrasensitive Nonisotopic Detection. Science. 281:2016–2018.

18. Mattoussi, H., J. M. Mauro, E. R. Goldman, G. P. Anderson, V. C. Sundar, F. V. Mikulec, and M. G. Bawendi. 2000. Self-assembly of CdSe-ZnS quantum dot bioconjugates using an engineered recombinant protein. J. Am. Chem. Soc. 122:12142-12150.

19. Medintz, I. L., H. T. Uyeda, E. R. Goldman, and H. Mattoussi. 2005. Quantum dot bioconjugates for imaging, labelling and sensing. Nature Materials. 4:435-446.

20. Smith, A. M., H. W. Duan, A. M. Mohs, and S. M. Nie. 2008. Bioconjugated quantum dots for *in vivo* molecular and cellular imaging. Adv. Drug Delivery Rev. 60:1226–1240.

21. Zhang, C-Y., H-C. Yeh, M. T. Kuroki, and T-H. Wang. 2005. Single-quantum-dot-based DNA nanosensor. Nature Materials. 4:826-831.

22. Hohng, S., and T. Ha. 2005. Single-molecule quantum-dot fluorescence resonance energy transfer. ChemPhysChem. 6:956–960.

23. Hyun, K. J., S. Chaudhary, and M. Ozkan, 2007. Multicolour hybrid nanoprobes of molecular beacon conjugated quantum dots: FRET and gel electrophoresis assisted target DNA detection. Nanotechnology 18:195105.

24. Dubertret, B., M. Calame, and A. J. Libchaber. 2001. Single-mismatch detection using gold-quenched fluorescent oligonucleotides. Nat. Biotechnol. 19:365–370.

25. Dyadyusha, L., H. Yin, S. Jaiswal, T. Brown, J. J. Baumberg, F. P. Booy, and T. Melvin. 2005. Quenching of CdSe quantum dot emission, a new approach for biosensing. Chem. Commun. 25:3201-3203.

26. Pons, T., I. L. Medintz, K. E. Sapsford, S. Higashiya, A. F. Grimes, D. S. English, and H. Mattoussi. 2007. On the quenching of semiconductor quantum dot photoluminescence by proximal gold nanoparticles. Nano Lett. 7:3157–3164.

27. Wargnier, R., A. V. Baranov, V. G. Maslov, V. Stsiapura, M. Artemyev, M. Pluot, A. Sukhanova, and I. Nabiev. 2004. Energy transfer in aqueous solutions of oppositely charged CdSe/ZnS core/shell quantum dots and in quantum dot-nanogold assemblies. Nano Lett. 4:451-457.

28. Algar, W. R., and U. J. Krull. 2007. Luminescence and stability of aqueous thioalkyl acid capped CdSe/ZnS quantum dots correlated to ligand ionization. Chemphyschem. 8:561-568.

Legends to Figures

Fig. 4.1. A schematic representation of the QD-MB-Au NP probe with or without presence of the complimentary viral RNA.

Fig. 4.2. Characterization of the QD-MB-Au NP complexes. (A) Fluorescence spectra of the QD-MB-Au NP complex at an increasing ratio of MB-Au NP conjugate from 1 to 6. Fluorescence spectra from 0.1 μM TOP/TOPO-capped CdSe-ZnS and DHLA-capped QDs are also shown. (B) The time profile of QD emission in the presence of 10-fold molar excess of a complimentary oligo.

Fig. 4.3. Tapping mode AFM analysis of the QD-MB-Au NP complex. (A) Open complex after hybridization with complimentary oligos (inserted images). The height profile of the open complex was obtained from the right image. (B) Closed complex without complimentary oligos (inserted images). The height profile of the open complex was obtained from the right image.

Fig. 4.4. Intracellular delivery of QD-MB-Au NP probes. (A) BGMK cells were incubated with the QD-MB-Au NP conjugates (50 nM) for 12 h, and fluorescent images were captured at different time points. (B) BGMK cells were incubated with QD-MB-Au NP conjugates without Tat modification.

Fig. 4.5. Detection of infectious viruses by QD-MB-Au NP probes. (A) Fluorescent images of cells infected with 0, 1, 10^2 or 10^3 PFU at 4 h post infection (p.i.). (B) The correlation between the number of fluorescent cells and PFU at 4 h p.i.

Fig. 4.6. (A) Real-time detection of viral spreading. BGMK cells were first incubated with 50 nM QD-MB-Au NP probes, infected with CVB6 at an M.O.I. of 0.1 PFU/cell, and monitored using a fluorescent microscope. (B) 12 h real-time monitoring by introducing 50 nM QD-MB-Au NP probes into the cells and no obvious false-positive fluorescent signals were observed (the merge images are shown).

Fig. 4.1.

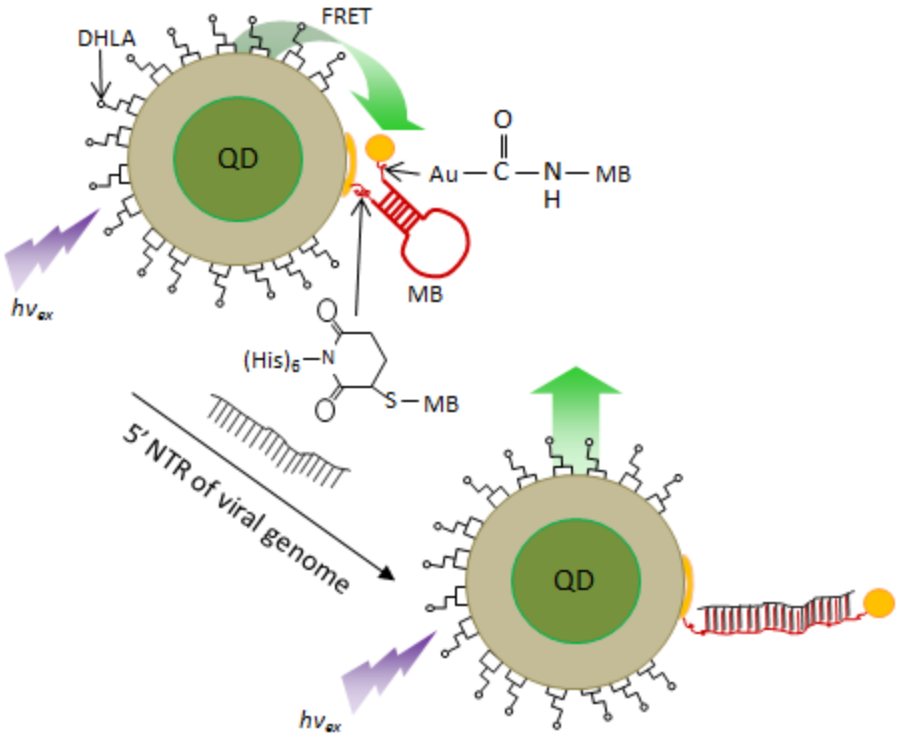
FRET
DHLA
QD
O
Au — C — N — MB
H
MB
hv_{ex}
$(His)_6$—N
S—MB
5' NTR of viral genome
QD
hv_{ex}

Fig. 4.2A.

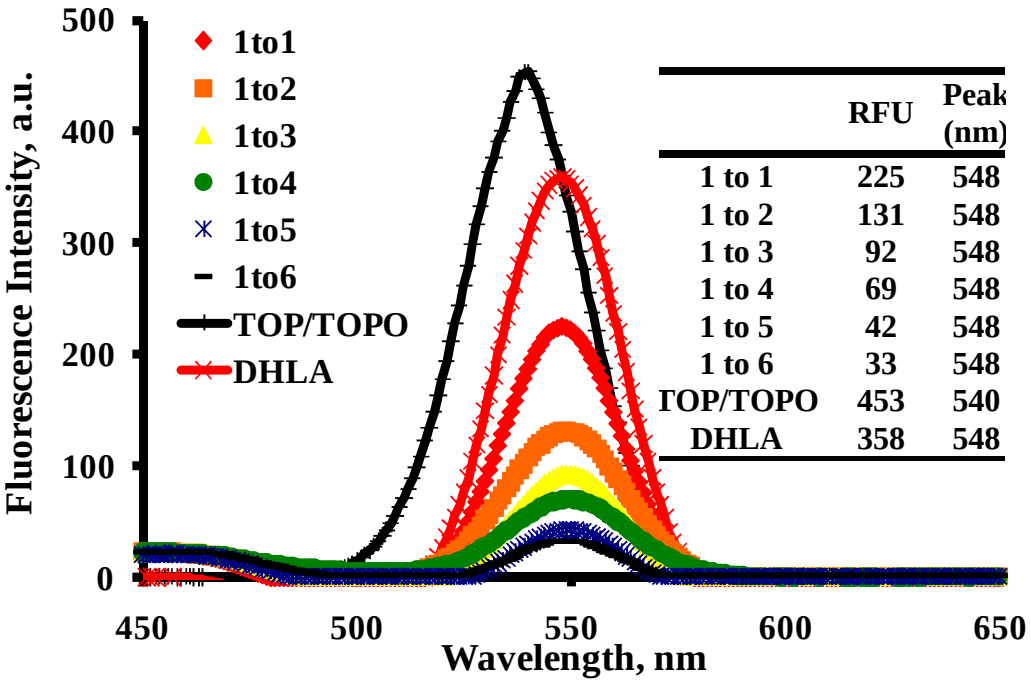

Fig. 4.2B

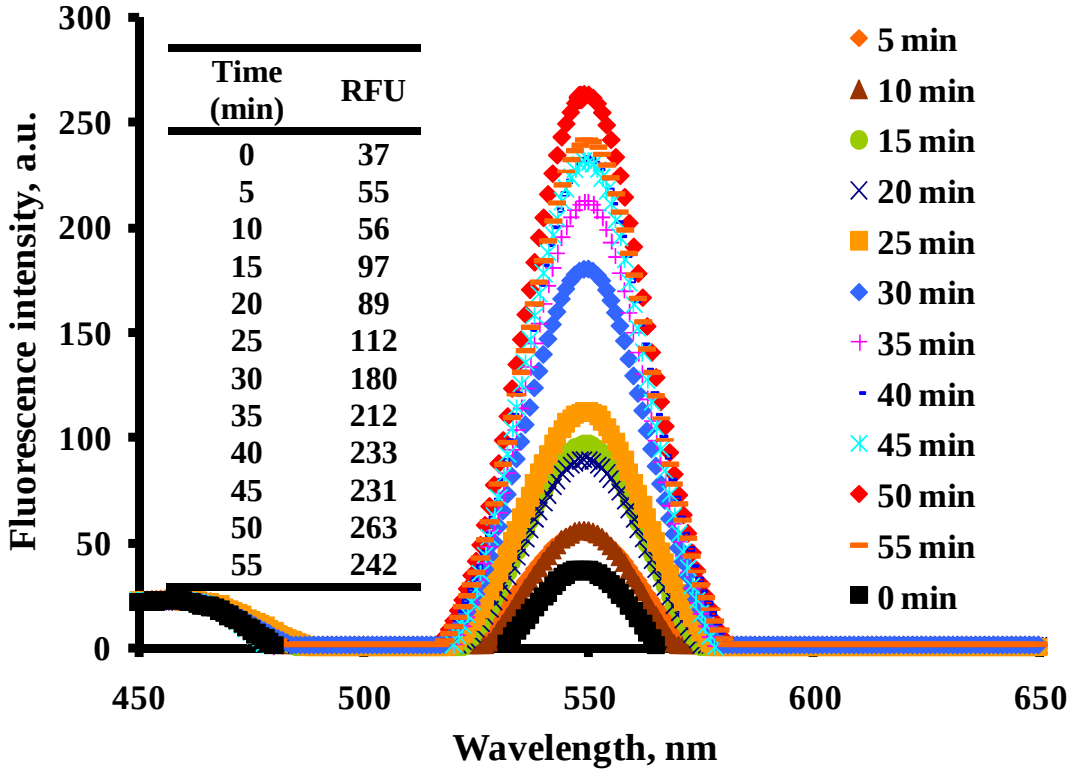

Fig. 4.3A.

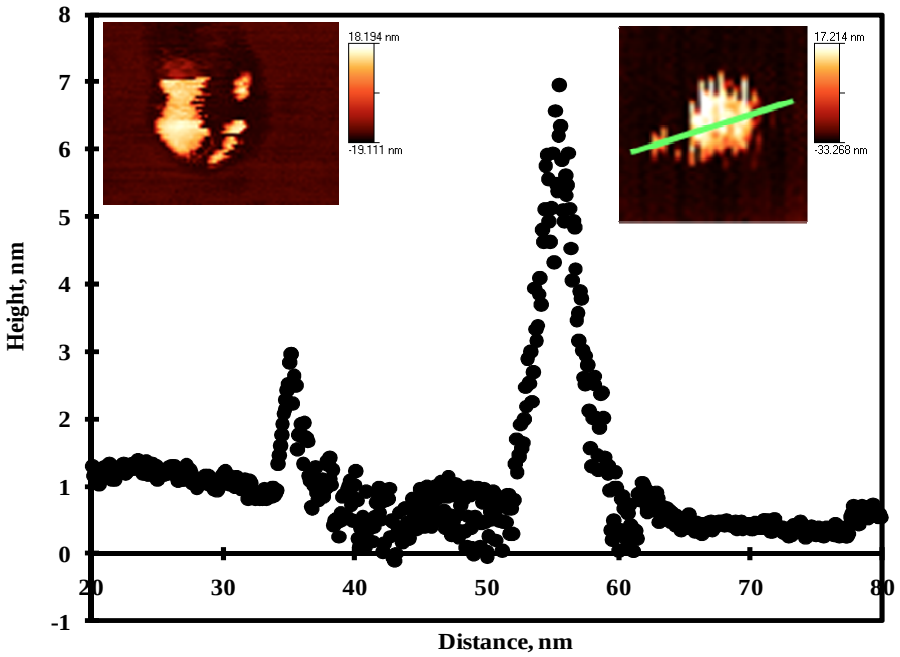

Fig. 4.3B.

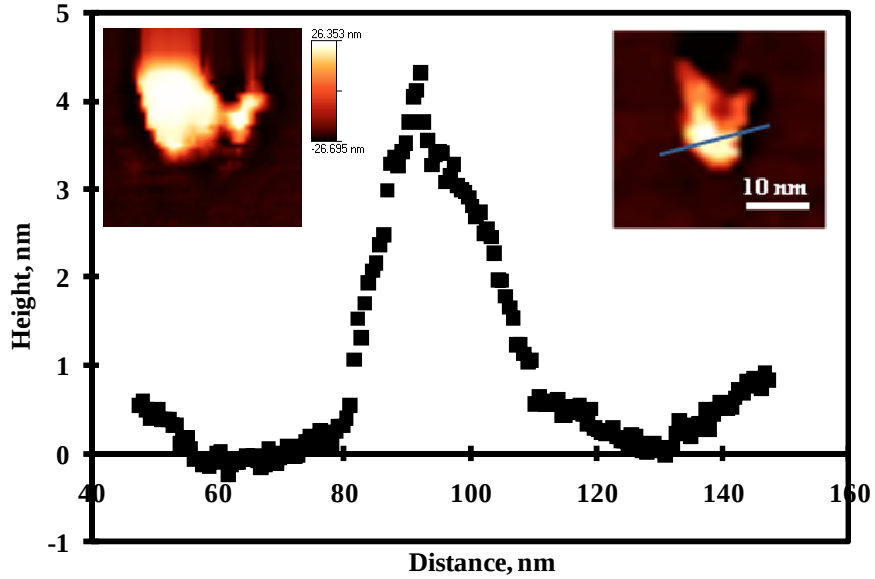

Fig. 4.4A.

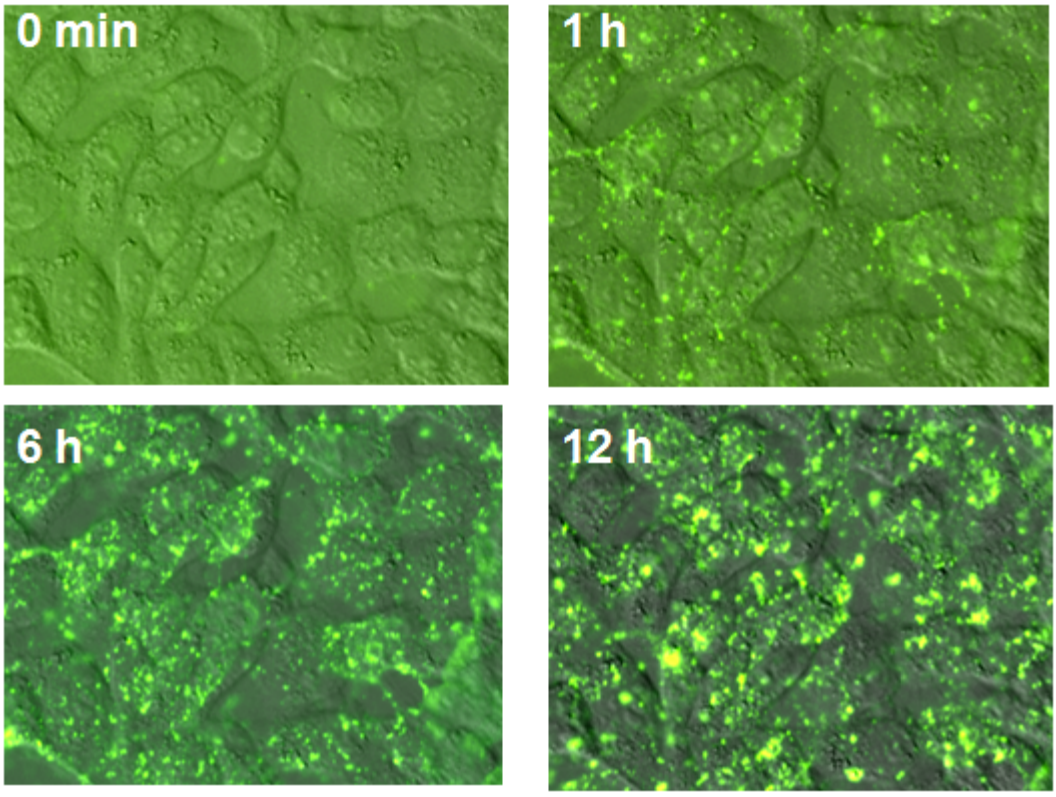

Fig. 4.4B.

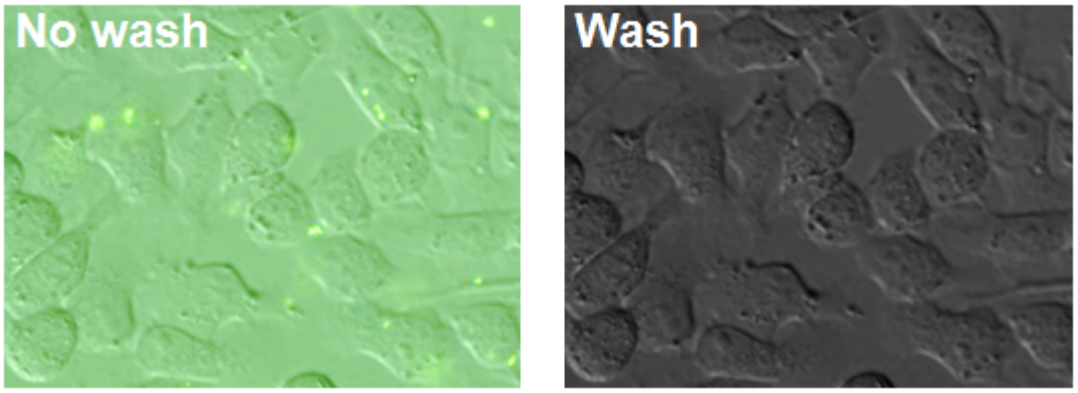

Fig. 4.5A.

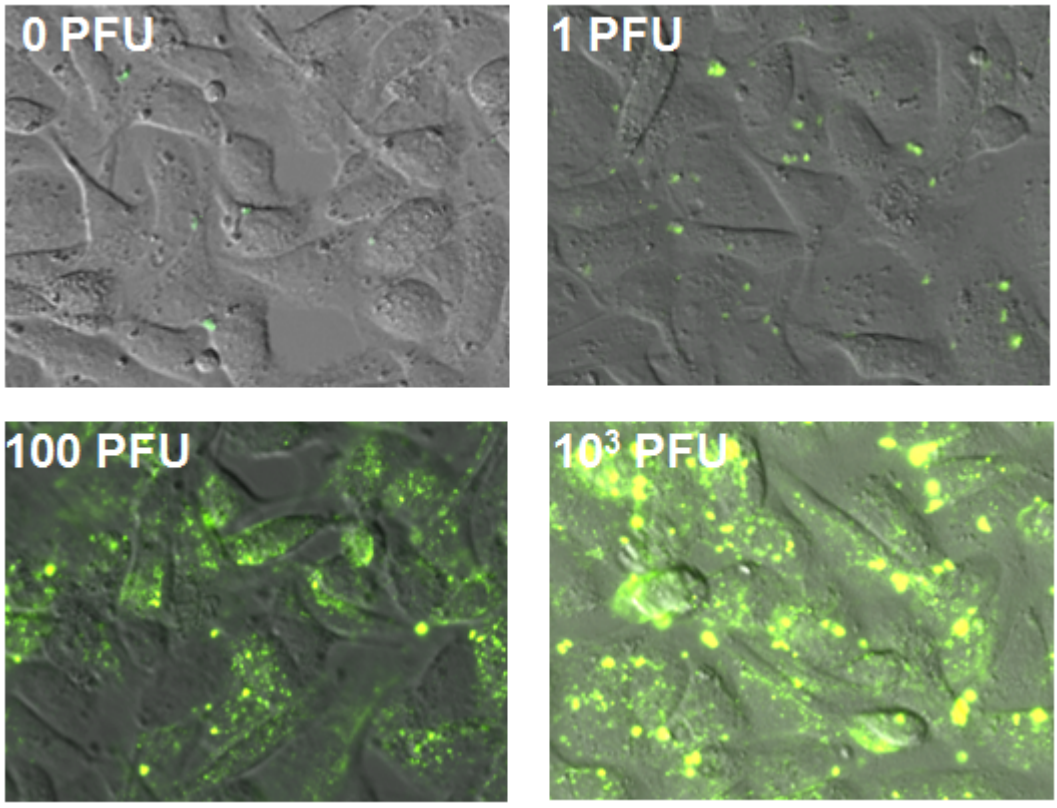

Fig. 4.5B.

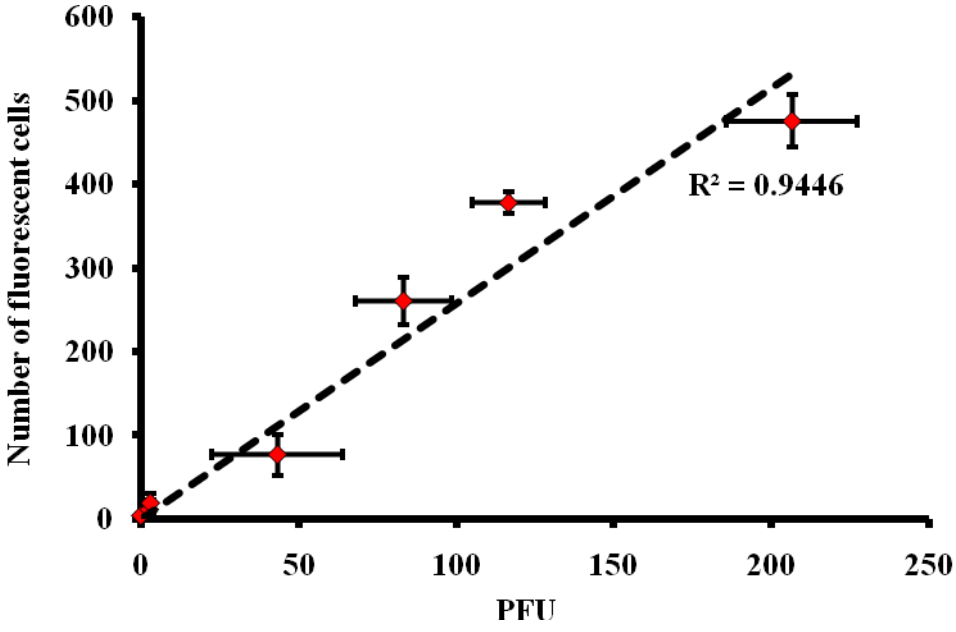

Fig. 4.6A.

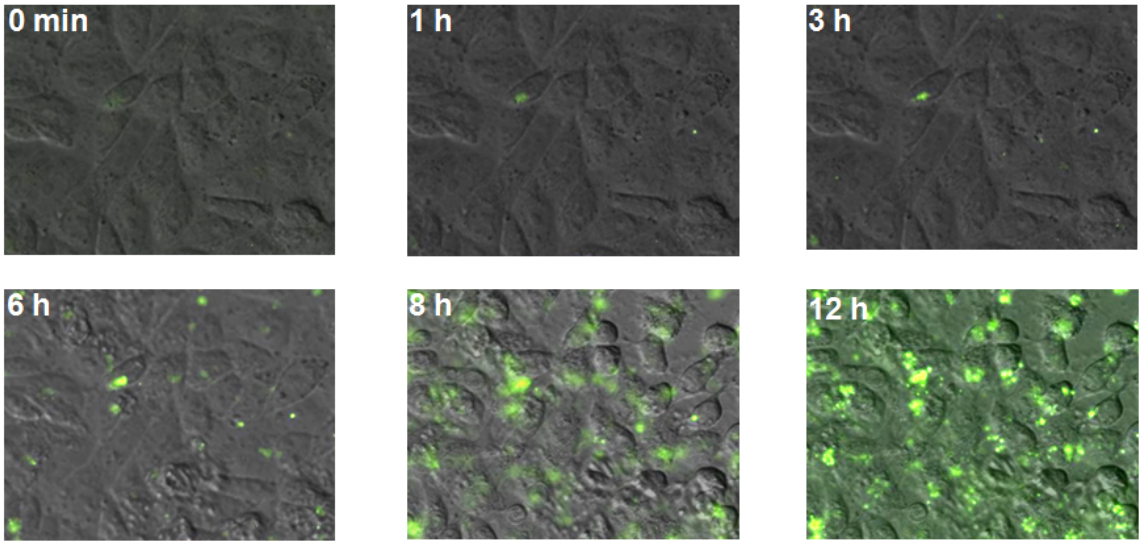

Fig. 4.6B.

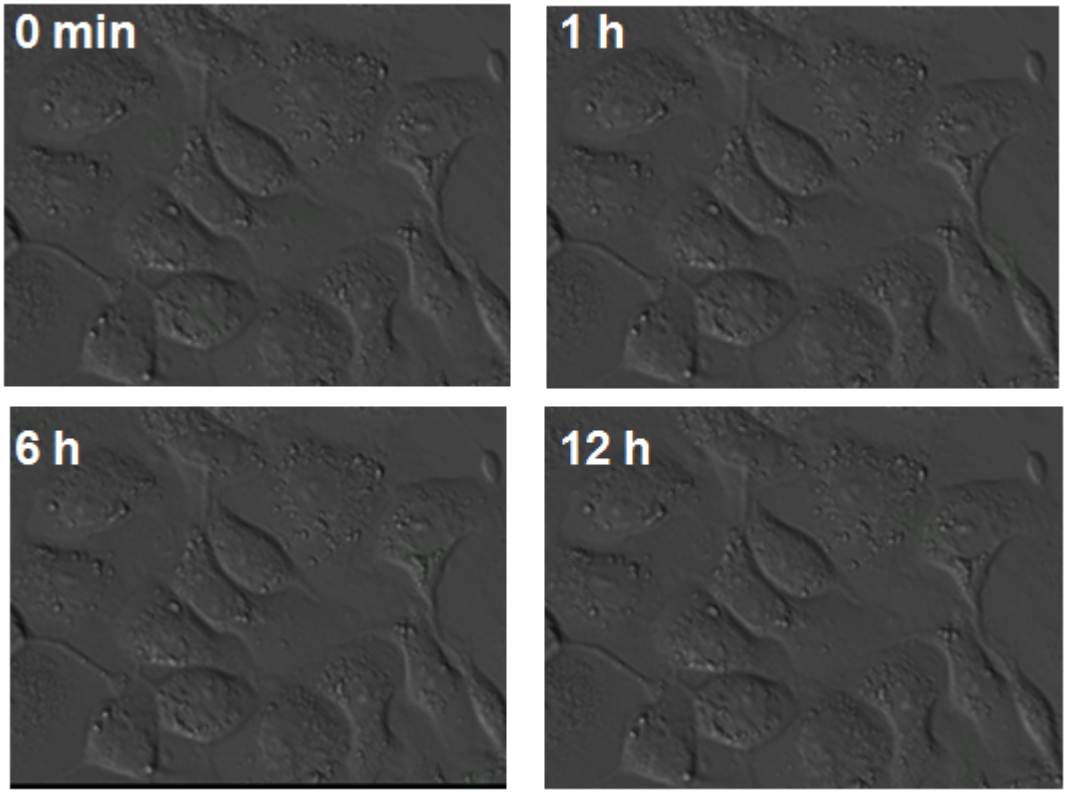

Conclusion

Waterborne transmitted viruses pose a public health threat due to their stability in aquatic environment and their ease of transmission with high morbidity rates at low infectious doses. Two major challenges of viral analysis include a lack of adequate information regarding infectivity and the inability to cultivate certain epidemiologically important viruses *in vitro*. The use of fluorescent probes in conjunction with fluorescence microscopy allows us to reveal dynamic interactions of the viruses with different cellular structures in living cells that are impossible to detect by immunological or PCR-based experiments. Real-time viral detection *in vivo* provides sufficient information regarding multiple steps in the infection process at a sub cellular level, which will be valuable for the prevention and control of viral infection.

In this study, we designed appropriate MB sequences that function optimally under the given assay conditions. The MBs (MB H1, MB CVB6-Tat and QD-MB CVB6-Au NP) demonstrated a high degree of specificity, which can be further applied to comparative studies of different subtypes of human enteroviruses. The data from our measurement can be collapsed to provide data equivalent to a plaque assay with a detection limit of 1 PFU, achieved within one replicative cycle. The fluorescence assay greatly reduces quantification time and produces infectivity information as a function of p.i. time points, which will benefit researches where the quantity of virus (production yields) at various steps is an important factor, such as the production of viral vaccines, MOI optimization and adaptation of methods to cell culture.

The improved elements of the detection techniques presented in this study are: (i) a nuclease-resistant backbone modification for prevention of nucleolytic degradation, (ii)

an attachment of the Tat peptide to the MB, to facilitate non-invasive entry into host cells, and (iii) a new FRET pair composed of QD and Au NP for improved sensitivity. The combination of nuclease-resistant constituents and the Tat peptide achieves an improved efficiency, i.e., real-time and long-term monitoring of viral infection without pretreatments (fixation and permeabilization). FRET microscopy was applied in this study to simultaneously track the viral genomes within host cells. It efficiently and rapidly captured the fluorescent signals from the MB-viral RNA interactions in living or fixed cells. By introducing the modified MBs (MB CVB6-Tat and QD-MB CVB6-Au NP) into the host cell population prior to viral infection and tracking the change in fluorescence intensity, we could observe cell-to-cell spread where progeny virions infected new host cells in which the infectious cycle could be repeated. The ability to monitor the real-time replication of viruses in living cells is vital for providing insights into viral pathogenesis and fundamental cellular functions and can lead to new therapies for combating viral infection. In the future, these novel MB-based probes can be utilized to empirically measure the constants of mathematical models for a better understanding of host-virus dynamics. By providing a mathematical expression to describe the biological process of host-virus interaction, fundamental viral proliferation studies can be elucidated from a combination of potential experiments and simulations. For epidemiologically important viruses that cannot be grown in cell culture, such as astrovirus or noroviruses, the Tat peptide can be used to introduce extract viral genomes into insusceptible cultured cells to permit one reproductive cycle. The use of modified

MB based probes could be used to demonstrate viral replication in cells proven to cultivate the virus.

Viruses will always remain a major health threat, and the inclusion of the techniques described above call for the development of multiplex approaches with the aim to detect and characterize several pathogens in a single assay. Furthermore, we have demonstrated the feasibility of turning the presented methods into tools to provide insight into the molecular mechanisms underlying the virulence of the viruses significant to public health. Ultimately, we hope this work will provide a link in the future efforts of developing antiviral treatments.